SURFACE EFFECTS OF BIOMACHINING PURE COPPER

By

Daniel Johnson

A Thesis Submitted to the Faculty of the

DEPARTMENT OF MECHANICAL ENGINEERING

In Partial Fulfillment of the Requirements

For the Degree of

MASTER OF SCIENCE

In Mechanical Engineering from

THE UNIVERSITY OF MICHIGAN

2 0 0 5

Committee Members:

Albert Shih
Associate Professor

Steven Skerlos
Assistant Professor

Table of Contents

List of Figures

List of Tables

Chapter 1. Introduction

1.1. Current Small-Scale Manufacturing and the Need for Improvement

The ever accelerating rate of progress in microelectronics has brought on an age of devices whose features are continually shrinking with each new generation. While the smaller scale of the circuits in these devices allows higher density and performance, it introduces new manufacturing, cooling, and material challenges that must be overcome. Perhaps the worst of these is the amount of heat produced that must be dissipated to prevent damage to the delicate metal traces. To help achieve this necessary goal, more and more manufacturers of integrated circuits are switching to using copper for their principle conductor, as copper has not only excellent electrical conductivity, but also one of the highest thermal conductivities of all pure metals.

Traditional manufacturing of microscopic patterns in copper involves a process called wet chemical etching. The pattern of circuits is first printed in negative onto the copper using photolithographic techniques. The part is then, typically, exposed to a solution of ferric chloride ($FeCl_3$), which can remove the copper at rates up to 234 μm/hr. [1] The samples are then simply rinsed and the photoresist is removed with another solvent, leaving the copper pattern on its substrate material.

While traditional chemical etching with ferric chloride is fast and effective, it has several drawbacks:

1. Ferric chloride works too quickly at eroding the metal for fine depth control. It is best used to remove all copper down to a substrate material that does not react with it. As future devices may utilize multiple three-dimensional features made out of copper, rather than uniform-depth monolayers, a slower, more controlled process is desired.
2. Ferric chloride, along with some other chemical etching techniques, also produces a very exothermic reaction, which can leave a heat affected zone on the surface of the metal being etched, and this can degrade the desired material properties of the metal. This is more of a serious issue for MEMs (micro electro-mechanical devices).
3. Ferric chloride is also toxic to both humans and the environment, posing many disposal problems.
4. Finally, as the process proceeds, the ferric chloride becomes less and less efficient due to the buildup of dissolved ions. While many processes have been invented to "regenerate" the ferric chloride and prolong the usable time of a given volume, ultimately it still ends up as a hazardous waste.

A more environmentally benign process in controlled etching of small-scale structures in copper is thus desired, especially as this area of the industry expands in the future.

1.2. A Biological Solution

One very promising solution to this problem comes from a recently discovered process known as "biomachining". Instead of using highly toxic ferric chloride or other chemicals to etch the copper, bacteria can be used to produce the same effect at a slower

rate and at lower temperatures, all for very low energy input and cost. If this process can be properly understood, controlled, and even accelerated (where desirable), it holds promise as a commercially viable alternative to chemical etching. The species involved and explanations of the underlying chemical processes are described in detail in section 2. Past experimental work is described in section 3, while experimental procedures and results of this study are elaborated upon in sections 4 and 5. Finally, conclusions and suggestions for future work are given in section 6.

Chapter 2. Overview of the Biological Mechanism Involved in Biomachining

2.1. Biological Background and Species Selection

Every organism can be classified based on where it obtains its carbon, used for growing and repairing damage, and how it produces energy, the fuel it uses to run all metabolic processes. Organisms known as *lithotrophs* obtain carbon from inorganic compounds, including carbon dioxide. *Organotrophs*, on the other hand, obtain all the carbon they use from organic compounds, including those from other organisms. Each of these groups can be further subdivided based on how included organisms obtain energy. The prefix *Chemo-* is given to those organisms that extract energy by processing matter, with *chemolithotrophs* typically processing inorganic matter, and *chemoorganotrophs*, which process organic matter. Many large animals (including humans) and bacteria are classified as chemoorganotrophs. The other energy production method involves using energy from light, and organisms that use this process have the prefix *Photo-* assigned to them. Plants are the most common examples of photolithotrophs.[2]

Organisms fitting into the category of chemolithotrophs have been the subject of intensive research lately for their unique ability to either oxidize or reduce certain inorganic compounds, especially heavy metals. Species such as *Shewanella oneidensis* have been investigated for a process known as "bioremediation" in which toxic chemicals are taken out of groundwater by the natural reduction reactions of the bacteria. Species such as *Geobacter metallireducens* and *Rhodoferax ferrireducens* have shown potential application for biologically-based fuel cells. Finally, species such as *Desulfovibrio sp.* and *Acidithiobacillus ferrooxidans* (formerly *Thiobacillus ferrooxidans*) have been shown to consume metals as part of their metabolism. This process, termed "biomachining", has been analyzed for potential applications to micro and nano-scale manufacturing, including for the potential processing of copper. *Acidithiobacillus ferrooxidans* shows the most promise of the two, both for its ease of culturing and pronounced consumption of the metal as it grows. A summary of the classifications, species, and potential applications is displayed below in Table 1.

Table 1: Classifications, species, and potential applications of various organisms

Carbon Source	Energy Source	Sample Species	Applications
Lithotroph (Carbon source: CO_2)	*Chemolithotroph* (Energy source: Inorganic matter)	*Acidithiobacillus ferrooxidans*	Biomachining [2, 3, 4, 5, 6, 7, 8] Bioleaching [9, 10, 11]
		Thiobacillus thiooxidans	Bioleaching [9]
		Geobacter metallireducens	Microbial fuel cells [12] Bioremediation [13, 14]
		Shewanella oneidensis	Bioremediation [15]
		Desulfovibrio sp.	Biomachining [16]
		Rhodoferax ferrireducens	Microbial fuel cells [17]
	Photolithotroph (Energy source: Light)	Plants, Chlorella, Cyanophta, etc.	N/A
Organotroph (Carbon source: Organic matter)	*Chemoorganotroph* (Energy source: Organic matter)	Humans, most animals, most bacteria	N/A
	Photoorganotroph (Energy source: Light)	*Rhodospirillaceae*	N/A

2.2. Basic Reactions of The Biomachining Process

The *Acidthiobacillus ferrooxidans* organism is a small, rod-like bacterium (shown below in Figure 1) measuring about 1 μm long and .5 μm in diameter [2] that contains a unique set of attributes that makes it suitable as a living micro-machining tool. This species belongs to a group of organisms known as chemolithotrophs, organisms (usually single-celled) able to obtain energy by the oxidation of inorganic substrates rather than the usual substances such as glucose. As a source of carbon, the organism can obtain all its needs solely by using CO_2 dissolved in its medium. Oxygen, serving as an electron acceptor, does have to be present to make these reactions possible, thus technically making *A. ferrooxidans* aerobic. The production of energy is obtained from the oxidation of the substrate as well as the combination of hydrogen ions and oxygen being fused into water. [18, 19] Finally, this bacterium is also considered an acidophile, as it is able to thrive in a pH level less than 3. [8]

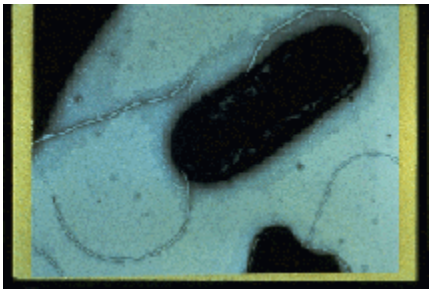

Figure 1: Acidithiobacillus Ferrooxidans [20]

The overall reaction employed by *A. ferrooxidans* can be summarized as a combination of the continued oxidation of ferrous iron (Fe^{2+}) to ferric iron (Fe^{3+}) as well as the reduction of H^+ ions (from the acidic environment) with oxygen to produce water. The reaction is shown below:

$$2Fe^{2+} + 1/2O_2 + 2H^+ \rightarrow 2Fe^{3+} + H_2O \quad (1)$$

It is the production of the ferric iron that makes this organism useful in micromachining of metals. The ferric iron is able to oxidize both pure, neutral copper and iron into charged, soluble forms, thus being able to corrode a solid surface of either metal. The reactions for each are summarized below:

$$Fe^0 + 2Fe^{3+} \rightarrow 3Fe^{2+} \quad (2)$$
$$Cu^0 + 2Fe^{3+} \rightarrow Cu^{2+} + 2Fe^{2+} \quad (3)$$

While the iron and copper ion creation reactions shown above in equations 2 and 3 occur outside the cell, those involved in the continuous production of ferric iron and water, shown in equation 1, occur inside the cell, as described below. [8]

2.3 Kinetics at the Cell Wall and Respiration

The cell of each *Acidithiobacillus ferrooxidans* has a cell wall made up of many layers that separates the interior of the cell, the cytoplasm, from its environment. The outer region of this wall consists of an outer membrane and a region called the peptidoglycan. This is then followed by a gap called the periplasmic space, where the pH of fluid inside the cell is still near that of the environment (usually ~2). Finally, an inner membrane separates the periplasmic space from the cytoplasm. The pH in this membrane increases to around 4.5, and in the cytoplasm, the pH approaches neutral. The reason for such marked pH variation is twofold: the oxidation of ferrous to ferric iron is easier to facilitate in lower pH environments, and an excess of hydrogen ions (i.e. a low pH) allows an ample source of reactant for the water production reaction. [7, 21] A representation of the cell wall is shown below:

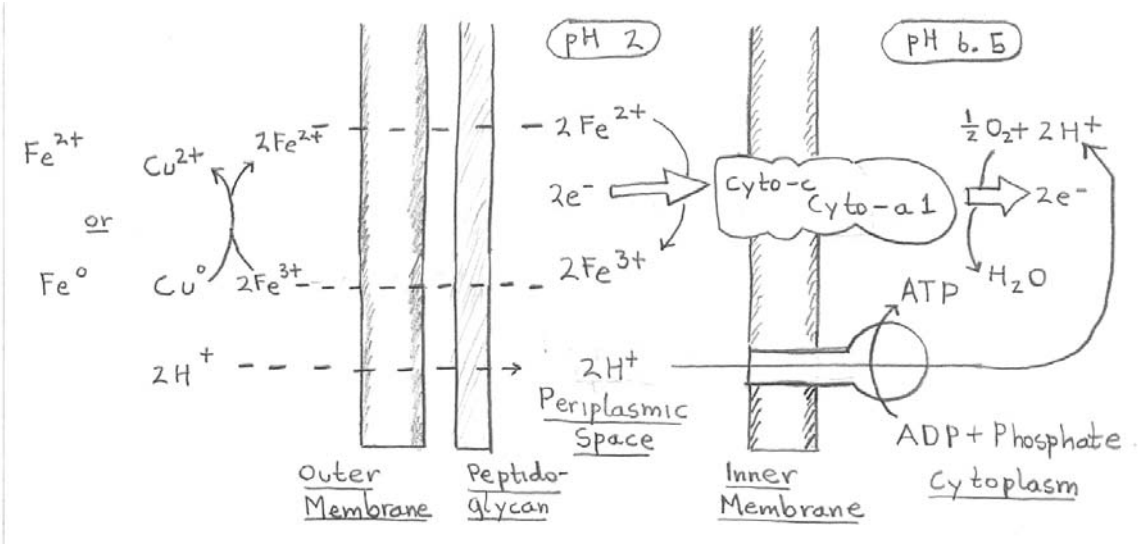

Figure 2:The Cell wall of A. ferrooxidans and Key Reactions [7]

The first part of these reactions, the continuous production of Fe^{3+} from Fe^{2+}, involves the transfer of electrons from the ferrous iron. This process is accomplished by a series of cellular compounds known as cytochromes, labeled cyto.-c and cyto.-a1 in Figure 2. These large molecules, imbedded in the inner membrane of the cell wall, often contain metallic atoms such as iron or copper that have a high affinity for accepting electrons. An example of a typical cytochrome is shown below.

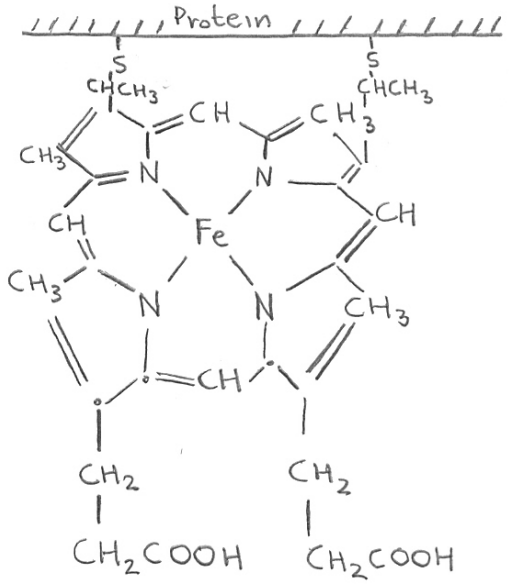

Figure 3: Cytochrome C Configuration [21]

In the process of stripping an electron from the iron atoms, these macromolecules are reduced. The electrons are then once again stripped by another cytochrome further in the cell, thus passing the electrons into the cytoplasm by a series of oxidation-reduction reactions. This group of cytochromes that strip and move electrons form what is called an "electron transport chain". In *A. ferrooxidans* we see cytochrome-c (which strips the

electrons from the iron ions) in combination with cytochrome-a1. [7] It is believed that cytochrome-a1 performs a similar task to another cytochrome in its family, called a3, which facilitates the reoxidation (taking the acquired electrons back out) of c-cytochromes, thus acting as a c-cytochrome oxidase. Cytochrome-a1 is believed to be the final link in the electron transport chain described above. It must be said, however, that the exact functioning of this group of cytochromes is still not well defined. [21]

The oxidation of iron takes place in the low pH of the periplasmic space along with the uptake of H^+ ions. The whole goal of these two processes, the coupling of the reoxidation of the cytochromes and the reactions of hydrogen ions with oxygen, is to produce useable energy for the organism. These reactions produce energy by virtue of the free energy change between the products and the reactants, and this energy is used to bind an extra phosphate onto the Adenosine diphospate molecule, thus creating Adenosine triphosphate. The actual efficiency of the cells in utilizing the redox reactions can vary from 10%-50%, but this is still efficient enough to produce the necessary energy to create ATP. [22] The ATP molecule is vital in nearly all organisms as a means of storing and transporting energy throughout the cell. It can store energy in the extra phosphate bond until needed by some cellular process, and then release it to create ADP and a free phosphate (which can then be recombined into ATP again). The phosphate bonds are theoretically able to hold anywhere from 37.656–58.576 kJ (9000-14000 calories) each, and for each atom of oxygen consumed in a reaction, 1-4 phosphate bonds can be produced. [21] Another theoretical calculation estimates that the overall reaction used by *A. ferrooxidans* produces around 33.472 kJ/mol (8 kcal/mol) of usable energy [2, 5]

The energy creating process forms a circulatory system of sorts for the iron ions as they are continually converted to Fe^{3+}, exuded from the cell, reduced to Fe^{2+} by their reaction with copper or iron, then reabsorbed into the periplasmic space for reoxidation. Hydrogen ions are obviously consumed and water is produced. Thus, H^+ ions must be continually supplied or the reaction cannot move forward. A representation of the reactions involved is depicted below in Figure 4:

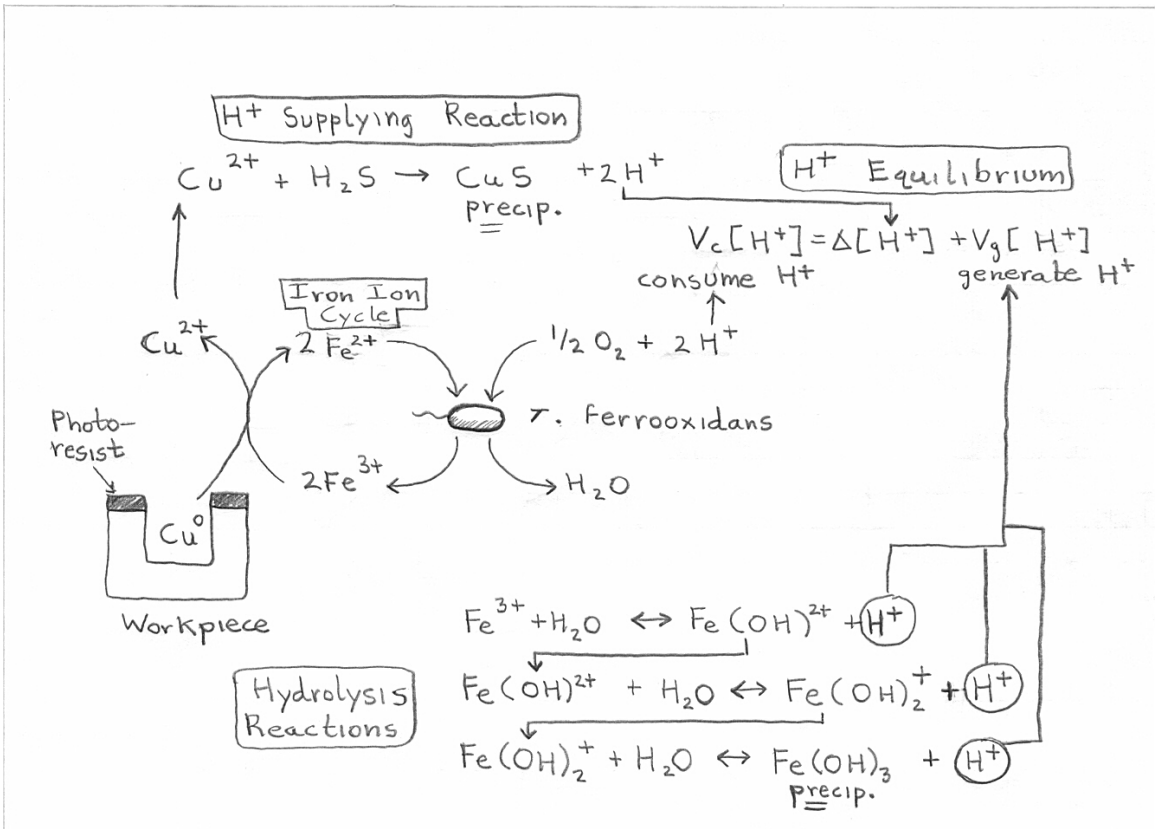

Figure 4: Biomachining Process Reactions [8]

The lower reactions on the chart come from the ferric iron ion's natural hydrolysis with water, ultimately producing $Fe(OH)_3$ and free H+ ions. It is in part due to this reaction that the ferric iron ion reaction with the workpiece material is best achieved by those bacteria actually in contact with the part surface. The H^+ supplying reaction, as labeled, is a consequence of the copper ions reacting with H_2S, which was added to the medium. The exact reason for using H_2S rather than some other H source is described below in section 3.2.

Acidithiobacillus ferrooxidans, through the complex reactions described above, is thus able to make the energy it needs to survive by performing a useful task to manufacturing engineers. Through the oxidation of pure iron and copper, this organism is able to produce a machining effect comparable to chemical etching. If all of the parameters of this biomachining process can be understood and controlled, it may become a commercially viable process able to compete with existing chemical etching in terms of productivity and yet be far more environmentally benign.

Chapter 3. Previous Work on Biomachining

3.1. Pioneering Work of Uno, Kaneeda, and Yokomizo.

One of the earliest studies of using *A. ferrooxidans* in a manufacturing capacity was performed by Uno, Kaneeda, and Yokomizo in Japan in 1993, as described in [2]. While employing a very basic experimental setup, they were able to show some preliminary data on the effects of changing some of the parameters involved in the biomachining process, and even suggest a way to accelerate the process with a properly-applied electric potential.

The setup first employed very pure samples of iron (99.95%) and copper (99.90%) which had line patterns put onto them by existing photolithography techniques. This left alternating sections of photoresist and exposed metal on the upper surfaces. The bacteria and the samples were immersed in a medium known as "9K", the ingredients of which are described below in Table 2:

Table 2: 9K Media Components [2]

Component	**Mass/10L Water**
$(NH_4)_2SO_4$	30 g
K_2HPO_4	5 g
$MgSO_4$	5 g
KCl	1 g
$Ca(NO_3)_2$	0.1 g
Deionized water	10 L
H_2SO_4	Adjust the pH to 2.5
$FeSO_4$	3 vol%

The samples and bacteria, immersed in the 9K medium and in open beakers, were then incubated at a constant temperature and constantly mixed with an agitator. The sketch of the experimental setup is shown below in Figure 5:

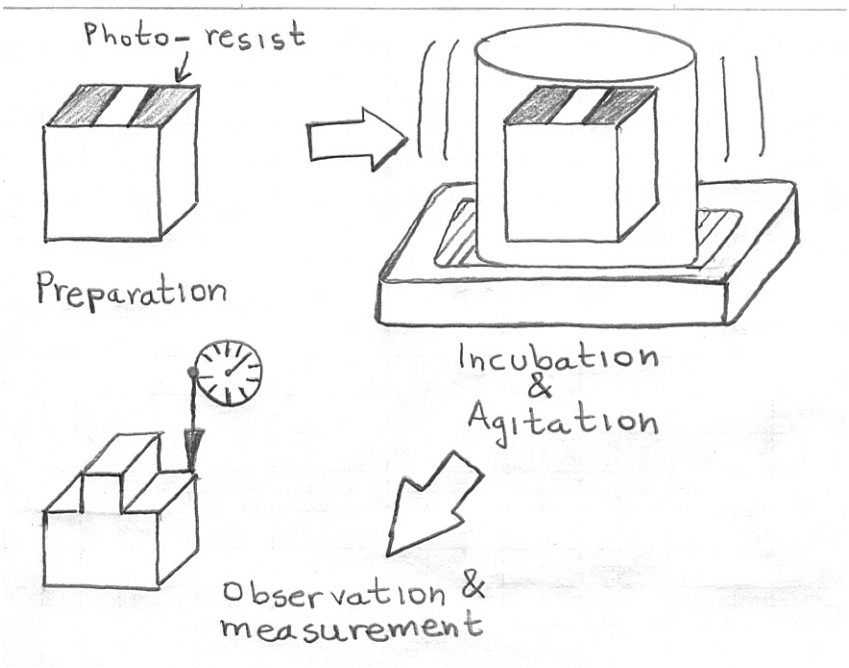

Figure 5: Basic Biomachining Experimental Setup [2]

The experiments were first run with a constant temperature of 28º C and a shaking rate of 160 cycles per minute. Three different strains of *Acidithiobacillus ferrooxidans* (ATCC 13598, 13661, and 33020) were tested in these runs on both metals, and all yielded similar results, as shown below in Figure 6:

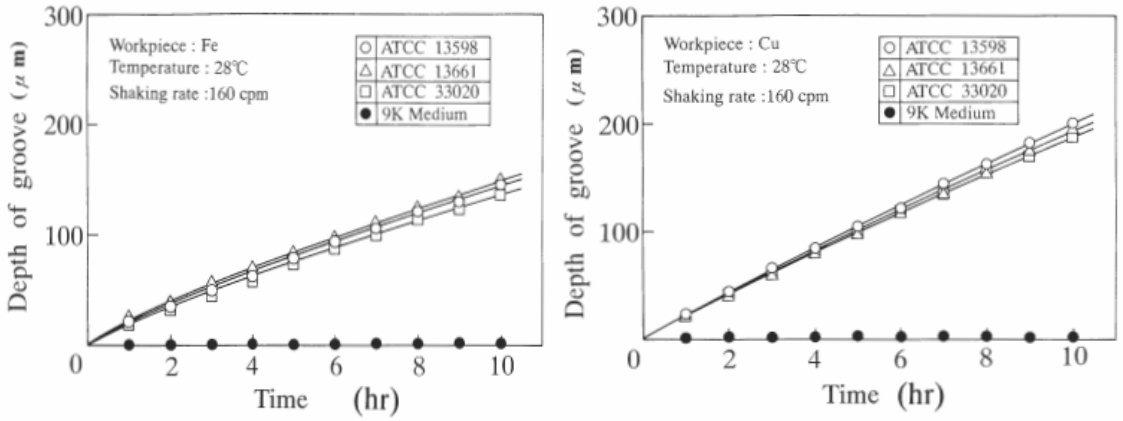

Figure 6: Biomachining Experiments on Fe (left) and Cu (right) [2]

As shown in the graphs, the biomachining rate at these conditions is almost directly proportional to time for all three species, which makes the process time relatively simple to predict. For Cu, the MRR was about 20 μm/hr, and for Fe the MRR was 14 μm/hr. The control of the experiment, using just the 9K medium, shows that the bacteria do indeed produce all of the material removal effect despite the corrosive (pH ~2.5) medium.

As a variation on the initial conditions, the researchers varied temperature for one strain (ATCC 13598) and observed the mean material removal rate. The results for both Fe and Cu are shown below in Figure 7:

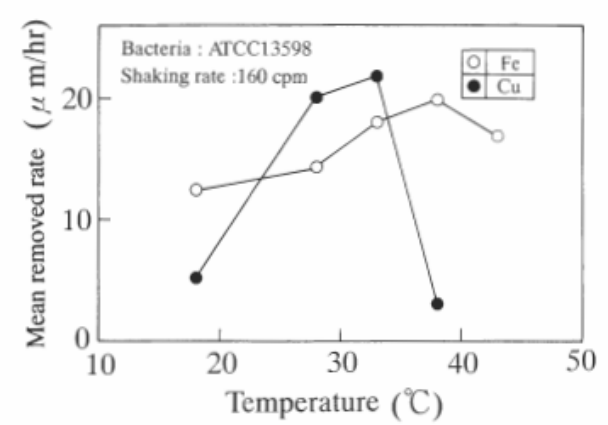

Figure 7: Mean MRR vs. Temperature in Biomachining [2]

As the figure shows, the peak MRR for Cu (~23 μm/hr) is near 30ºC, while for Fe, the max MRR (~20 μm/hr) occurs near 40ºC. Thus, temperature proves to be a relatively key variable in the efficiency of biomachining. Any process designed to employ biomachining will obviously have to control temperature to keep the MRR near its theoretical maximum.

As a final experiment with biomachining, Uno et al. applied different electric potentials to the workpieces to observe how changing that would influence the biomachining rate. The results for using strain ATCC 13598 on Fe and Cu for a variety of applied voltages are shown below in Figure 8:

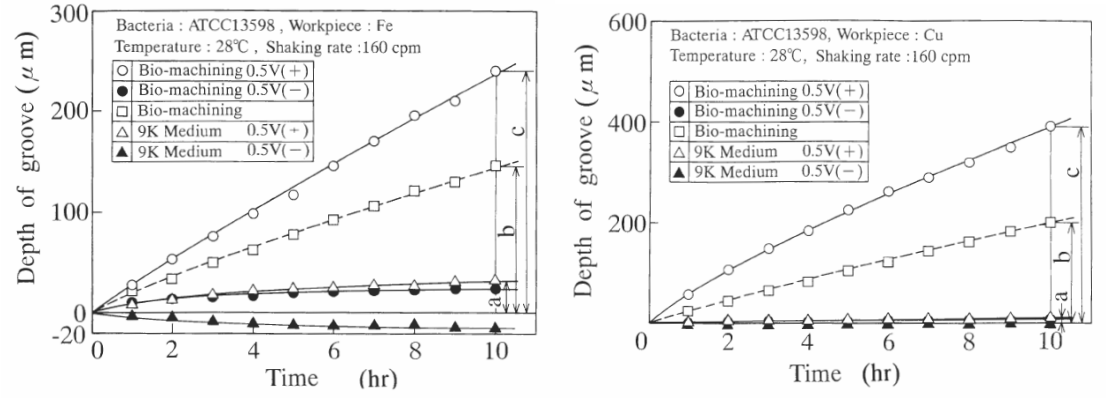

Figure 8: Biomachining with Varied Applied Voltages for Fe (left) and Cu (right) [2]

As shown above, if positive applied voltages are used, the MRR is accelerated over baseline. For iron, if the voltage applied is negative (.5V in this case), the MRR is actually negative, indicating material is deposited. Thus, applied voltage can have an accelerating effect in the biomachining rate, but more work needs to be done to determine if there is a maximum voltage which yields a benefit to the process.

3.2. The work of Zhang and Li: Mechanisms and Kinetics

Another pioneering group in the area of biomachining worked in China, producing papers on the subject in 1996 and 1998.[7, 8] Zhang and Li not only elaborated on the biological mechanisms used by *A. ferrooxidans*, but also gave equations relating the kinetics of the overall reaction to experimental conditions. Their more detailed work can give us valuable insight into the process and an initial point to begin studying parameter adjustment in the biomachining process.

In their 1996 paper, Zhang and Li perform an experiment very similar to the one by Uno, et al. The sample was prepared once again using existing photolithographic techniques. The prepared sample was then incubated with the bacteria for a period of time. Finally, the sample was removed periodically and measured both with a profilometer and scanning electron microscope. The data they collected showed that the average biomachining (i.e. material removal) rates were 10 μm/hr for iron, and 13.5 μm/hr for pure copper. The data graphs producing these rates are shown below in Figure 9:

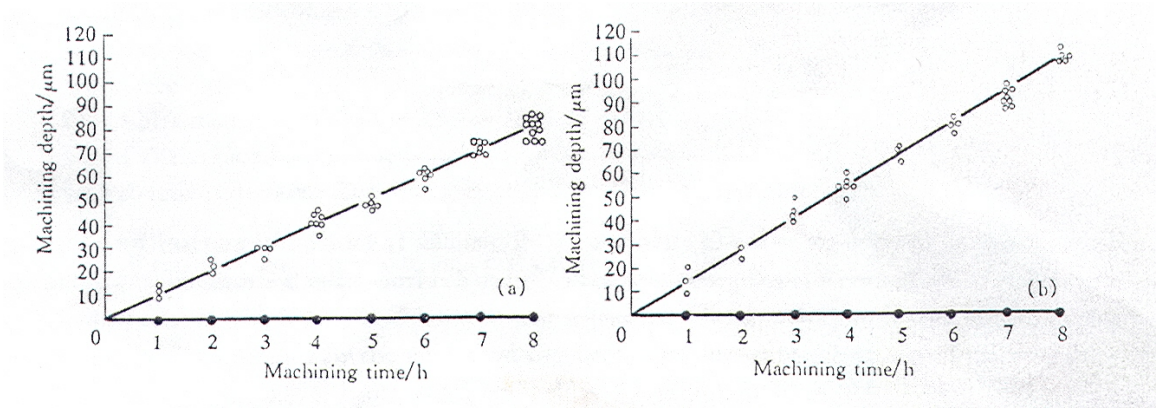

Figure 9: Biomachining Depth vs. Time for Fe (left) and Cu (right) [7]

As figure 9 shows, the biomachining rates in Zhang and Li's tests remained nearly constant over the length of the tests. In addition to this, Zhang and Li explained the Fe oxidizing and reducing reactions involved, as used above, as well as explaining what parts of the cell (periplasmic space, cytochromes, etc.) are used in the reactions. They concluded that the biomachining process is entirely dependent on the biological recreation of Fe^{3+}.

In 1998, Zhang and Li went further in explaining the biomachining process by studying the kinetics of each sub-reaction and how experimental concentrations affected each of these reaction rates. The first reaction relates the consumption of Fe^{3+}, labeled as $Vc[Fe^{3+}]$ below in equation 4, to the mass change of a Cu sample:

$$Vc[Fe^{3+}] = 2 * \Delta Cu^{0} * 10^{4} / 63.54(mmol/(L * h)) \quad (4)$$

After this, the rate of generation of Fe^{3+} (shown below as $V_g[Fe^{3+}]$ in equation 5) is dependent on both its consumption (denoted as $V_c[Fe^{3+}]$ below) and what Zhang and Li called its "increase rate" ($V_t[Fe^{3+}]$):

$$V_g[Fe^{3+}] = V_t[Fe^{3+}\} + V_c[Fe^{3+}](mmol/(L*h)) \quad (5)$$

$V_g[Fe^{3+}]$ and $V_c[Fe^{3+}]$ tend to become equal over time, and $V_t[Fe^{3+}]$ starts out large in the first few hours of an experiment and then turns to zero as the system reaches a stable ion concentration. The equilibrium equations of generating and consuming Fe^{3+} show that these quantities are directly proportional to the Fe^{2+} and Fe^{3+} concentrations, respectively.

$$Kg = \frac{V_g[Fe^{3+}]}{[Fe^{2+}]} \quad (6)$$

$$Kc = \frac{V_c[Fe^{3+}]}{[Fe^{3+}]} \quad (7)$$

Kg (equation 6) is the rate coefficient of generating Fe^{3+} and Kc (equation 7) is the rate coefficient of consuming it. Both have units of mmol/(L*h).

In their experiments, Zhang and Li found that the generation and consumption rates and coefficients were directly proportional to bacterial cell concentration. The data for these rates, taking out effects of non-biological sources and sinks of Fe^{3+} are shown below:

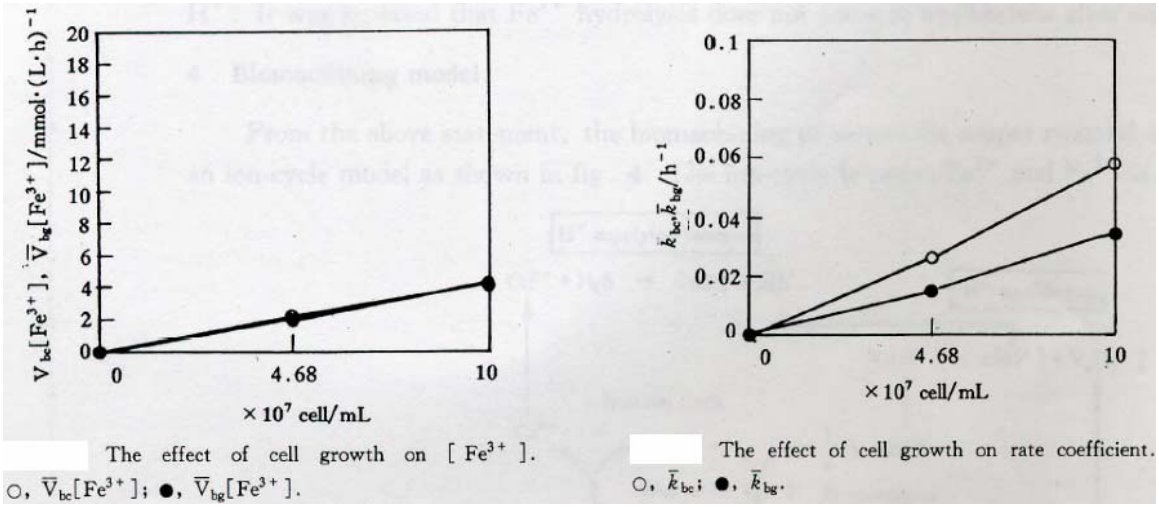

The effect of cell growth on [Fe^{3+}]. ○, $\bar{V}_{bc}[Fe^{3+}]$; ●, $\bar{V}_{bg}[Fe^{3+}]$.

The effect of cell growth on rate coefficient. ○, $\bar{k}_{bc}$; ●, $\bar{k}_{bg}$.

Figure 10: Vg[Fe3+]and Vc[Fe3+] vs. cell concentration (left) and Kg and Kc vs. cell concentration (right) [8]

The result of all of this is that the material removal rate is directly proportional to the amount of *A. ferrooxidans* organisms present, as might be expected. What these graphs don't show is whether or not there is some maximum bacterial concentration at which biomachining can occur. This leaves an open question for our research, as one obviously cannot increase the bacterial count indefinitely.

In their experiments, Zhang and Li studied how the hydrolysis of Fe (as described above in section 2) affects H+ ion concentration, which also affects the biomachining

process since it is taken up by *A. ferrooxidans* in the respiration process. They found that the natural decrease due to hydrolysis was lower than that caused by consumption by the organism. The big conclusion of the experiments is that H+ ions must be supplied to keep the reaction moving and allow the organism to reproduce/grow. Ideally, the pH should be kept around 2 to not negatively impact the process.

A final conclusion reached by Zhang and Li is that the buildup of Cu ions in solution (from their oxidation by Fe^{3+}) can cause the biomachining process to slow down. As shown in the schematic diagram of the reactions used above, they took care of this problem by bubbling H_2S gas into the solution. This gas supplies H+ ions and creates CuS, which precipitates, thus removing the Cu ions from solution.

Chapter 4. Experimental Setup

4.1. Introduction

To conduct our own experiments with *A. ferrooxidans*, the bacteria first had to be obtained and cultured successfully. Several variations on the basic liquid media for this species were tried until one that was both effective and easy to make was found. Before continuous cultures could even be created, however, the bacteria first had to be isolated, which is most easily done on solid media, such as common bacterial agar. Due to the acidic conditions required by this bacterial species, a specialized form of gelatinous media had to be found that would solidify even under a low pH. Finally, once we were confident we had isolated *A. ferrooxidans* and were able to continuously culture it, we had to devise a successful way to estimate bacterial concentrations.

Once the bacteria were successfully isolated and growing, an experiment was conducted to expand on some of the work described above done by early researchers in the field. For nano and micro-scale machining tasks, a high degree of precision is required to make any kind of material removal process successful. While Zhang, Li, and others were able to show that using an active population of *A. ferrooxidans* could remove a significant amount of material from a copper surface, they did not go into any detail on the resulting surface, and specifically its finish. For any process that may arise out of using these bacteria to machine copper, being able to produce level, even surfaces is highly desired. The experiments thus conducted by the author, as described in detail below, looked at changes in surface finish and roughness for several copper sample pieces. Both quantitative average roughness values and qualitative surface descriptions were obtained and are discussed below. All of the experiments show that, without some significant changes to the basic biomachining process, surface finish quality degrades significantly, and even though drastic material removal can be seen, the uneven nature of its distribution across a given surface makes direct applications in manufacturing seem doubtful.

A second experiment was conducted to obtain a crude estimate of the material removal rate of biomachining pure copper surfaces, in the hopes of replicating previous results. In that experiment, very thin copper foil pieces were exposed to solutions of *A. ferrooxidans*, as well as sterile media, for the same time periods as the copper blocks. The difference in mass was recorded and converted into a material removal rate using known material properties.

The experimental procedures used to observe the effects of *A. ferrooxidans* on surface roughness and material removal rates of the copper samples involved many steps and many different pieces of laboratory equipment. The combination of experimental steps and the continuous culture protocol employed to maintain a healthy population of the bacteria is summarized in the flow chart below (Figure 11), and a full list of equipment used appears in the subsequent table (Table 3). Detailed explanations of each step are laid out in the following sections.

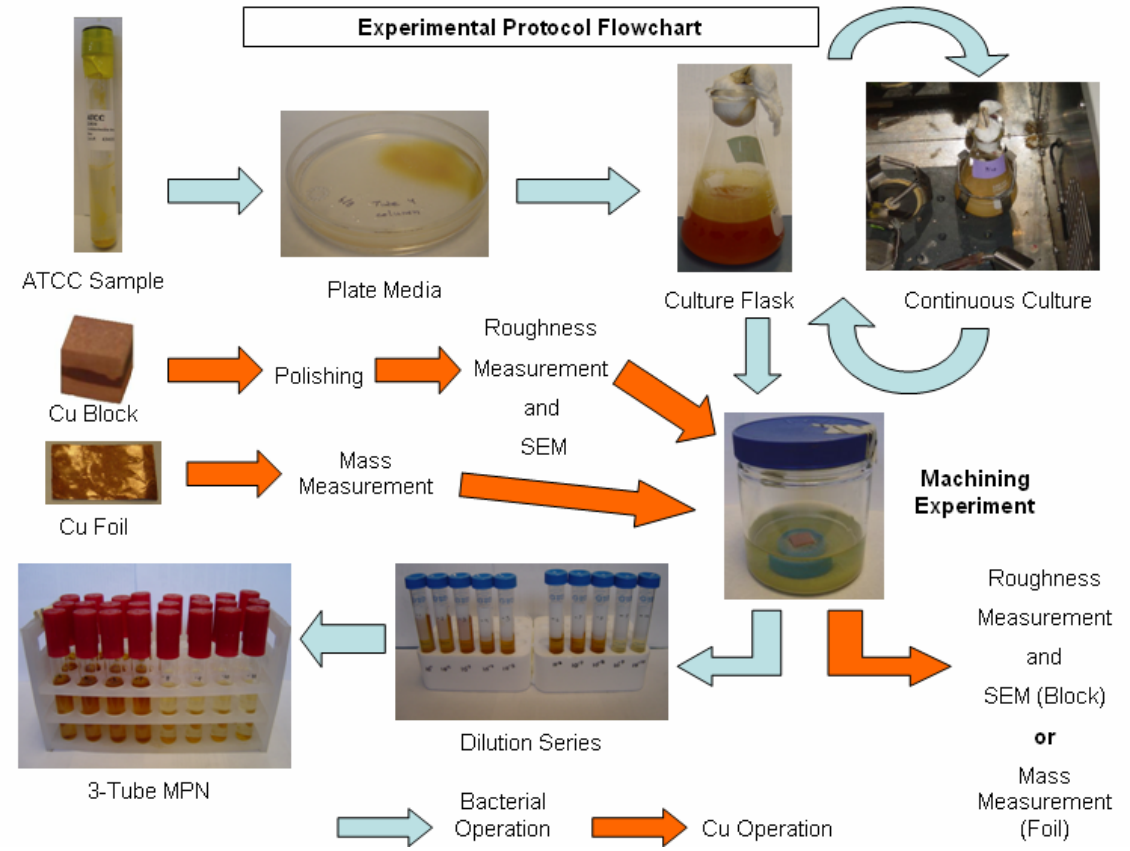

Figure 11: Experimental Procedures Flow Chart

Table 3: List of Equipment with Model and Manufacturers

Chemicals:	Stock distributed by Sigma
Incubator and Shaker:	innova 4300 by New Brunswick Scientific
Microbial Hood:	BioGARD Hood, by Baker Company, Inc.
Media Filtration System:	Stericup Pre-Sterilized Vacuum Driven Disposable Filtration System, .2 µm filter, 1L Jar by Millipore
Culture Flasks:	Pyrex 250 mL Erlenmeyer Flasks distributed by Sigma
Experiment Jars:	500 mLWide-Mouth Short Clear Glass Jars distributed by Fisher
MPN Test Tubes:	Fisherbrand Disposable Culture Tubes, Borosilicate Glass by Fisher
Dilution Series Tubes:	Falcon Blue Max Jr. 15 mL Polypropylene Conical Tubes by Becton Dickinson
Plates:	Fisherbrand 15mm Cell Culture Plates by Fisher
Flask Filter Top:	Fisherbrand Non-Sterile Cotton Gauze Sponges by Fisher
Copper Foil:	Copper Shim Stock (110 Annealed) by Lyon Industries
Copper Stock:	Alloy 101 Extreme-Temperature Electronic-Grade Copper distributed by McMaster-Carr
Profilometer:	Talysurf Intra by Taylor-Hobson
SEM:	XL30 by Philips
Mass Scale:	PG802-S by Mettler Toledo
pH Meter:	Φ360 by Beckman

4.2. Bacterial Media

For any microorganism to be able to grow and reproduce successfully, it must be kept in an environment that contains all of the nutrients and environmental conditions it requires to live. *A. ferrooxidans*, as described above, typically requires a liquid environment with a low pH and some metal to serve as its source of electrons in the respiration process. This particular species has been known to biologists for some time, so there are standard media recipes available for it and other similar acidophilic bacteria. The most commonly used media is referred to as 9K, which is a rather simple mix of salts and sulphate compounds combined with a source of iron for use by the bacteria.

4.2.1. Liquid Media

The most basic recipe found for 9K bacterial media was used based on that listed at the website of All-Russian Collection of Microorganisms.[23] This recipe employs two separate solutions that are mixed after sterilization. Each component is added in the order listed.

Table 4: 2-Solution 9K Media Components [23]

Solution 1	Solution 2
700mL H_2O	300mL H_2O
0.1g KCl	30g $FeSO_4 \cdot 7H_2O$
3g $(NH_4)_2SO_4$	
0.5g $Mg\ SO_4$	
0.5g $K_2\ PO_4$	
0.01g $Ca(NO_3)_2$	

The pH of each is adjusted to 2.5-2.6 using sulphuric acid (H_2SO_4). Finally, each solution is passed through a .2 µm filter into a sterile, sealed flask. When the two solutions mix in the flask, the mixture becomes opaque and yellow, and a precipitate forms. The precipitate eventually oxidizes even in the sealed flask, rendering the media less useful for bacterial culture of *A. ferrooxidans*. The approximate shelf-life of this 9K media is two to three weeks.

4.2.2. Solid Media

Solid media was used for isolation of *A. ferrooxidans* after first obtaining samples from ATCC. This plate media incorporated three solutions that were combined at the time of pouring. The solution formulations (as originally given) are shown in Table 5:

Table 5: Solid Media Solution Components [24]

Solution 1	Solution 2	Solution3
10g $Fe\ SO_4$	0.9g $(NH_4)_2SO_4$	1g/100mL Bacterial Agar
500mL H_2O	0.35g $Mg\ SO_4$	
	0.175g Tryptone Soy Broth	
	500mL H_2O	

Solutions 1 and 2 each had their pH adjusted to ~2 using H_2SO_4. Instead of TSB, Bacto Tryptone was used and desired results were still achieved. After experimenting with several ratios of the solutions, we found a 1:14:10 combination of solution 1:solution 2:solution 3 worked very well. Further increasing the proportion of agar solution produces a media that solidifies very well, despite the acidic nature of the other solutions. Plates using this media were poured under a bacterial hood to ensure sterility.

4.3. Culturing A. ferrooxidans

The bacterial sample came directly from ATCC (#21834) in a sealed test tube, as shown below in Figure 12.

Figure 12: A. ferrooxidans sample as-shipped from ATCC

After acquiring the initial sample from ATCC, 2 mL of sample broth were directly deposited onto plate media. Samples were then left to incubate at 35° C until bacterial colonies became visible. The colonies that did appear were extremely small units almost impossible to see except under high optical magnification. To the naked eye, bacterial growth appeared as a bright yellow, almost-transparent cloud on the surface of the media, typically arranged as one large mass. A typical plate with growth is shown below in Figure 13.

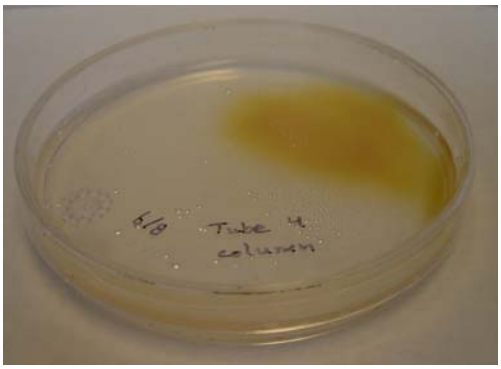

Figure 13: Plate Media with Growth (Upper-Right)

To further isolate *A. ferrooxidans*, streaks were taken off of the growth on the plates using sterile plastic picks and mixed into 15mL conical tubes of liquid 9K media. After one or two days of being incubated, again at 35°C, bacterial growth appeared as a drastic color change of the media, which turned a bright orange and developed an iridescent film at the surface. The precipitate also turned a dark orange color. As a control, blank tubes of sterile 9K media were incubated at identical conditions. The controls showed almost no change, with the usual light yellow precipitate color only darkening slightly as it oxidized. A side-by-side comparison of the media exhibiting growth and a control sample is shown below in Figure 14.

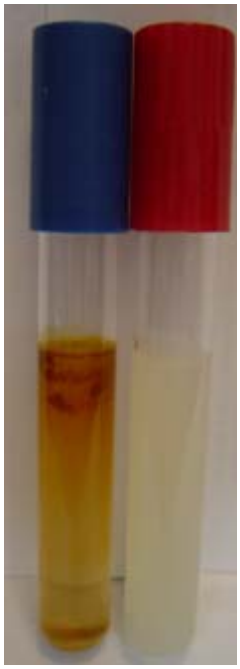

Figure 14: Example Tubes with Bacterial Growth (left) and Without (right)

Continuous cultures of *A. ferrooxidans* were produced by taking several mL from tubes showing the most dramatic signs of growth and mixing them into flasks of 9K media. Each flask was created with a vented top of tightly packed medical gauze which was covered with aluminum foil and autoclaved. Each 250 mL flask was filled with 150 mL of 9K media upon use, and after the bacterial broth was mixed in, the vented tops

were replaced, all under a bacterial hood to avoid contamination. The inoculated flasks were then incubated at 35°C and shaken at 120 cycles/minute. Using this culturing protocol, one flask would last approximately four to seven days, at which time the process was repeated using 2 mL from the previous flask.

The growth behavior visible in the shaken flasks was very similar to that mentioned for the sealed conical tubes used in isolating the bacteria. The 9K media generally turned a bright orange color within two days (Figure 15), and the precipitate solidified into one darker mass on the bottom of the flask. As time passed, the color would fade back to almost the same light yellow color of uninnoculated 9K media, but the precipitate would remain as one hard, solid mass on the bottom (Figure 16). Generally, this reversal of the color change would happen after four to five days, and that was used that as an indicator of when to create a fresh inoculation. As a control, sterile 9K media was again incubated under identical conditions, and just like in the tube controls, only a slight darkening of the precipitate was observed after many days due to oxidation.

Figure 15: Culture Flask After ~48 Hours Incubation (2mL Innoculation)

Figure 16: Culture Flask After ~120 Hours Incubation (2mL Innoculation)

4.4. Bacterial Concentration Estimation Technique: The 3-Tube MPN

Due to the small size of *A. ferrooxidans* cells, conventional counting techniques that rely on optical microscopy were deemed ineffective for estimating the bacterial populations in the biomachining experiments. Instead of using a device such as a hacyometer to count individuals present in a pre-determined fluid volume by visual inspection, a statistical method known as the most probable number (or MPN) technique was used that could give very clear results with reasonable levels of accuracy.[25, 26] This technique involves two main steps: creating an initial series of dilutions of the original sample, and then using those dilutions to inoculate a collection of test tubes to watch for growth.

Starting with an initial bacterial sample, in this case broth incubated for 48 hours, the first step in creating an MPN is to create a collection of dilutions of that initial sample. Initially, one mL of original sample is put into a test tube containing 9mL of sterile media of the same type used in culturing the bacteria. The resulting 10 mL solution is then a 1:10 dilution of the original bacterial solution. To create the next dilution, 1 mL of the new solution is withdrawn and put into a second tube of 9 mL of sterile media. The second tube, now with 10 mL of solution, is now a 1:100 dilution of the original sample. Each subsequent transfer of 1 mL to a fresh tube of 9 mL sterile media creates another power of ten dilution of the original bacterial sample. In this

manner, the original solution can be diluted as many times as is believed to be necessary. A typical dilution series is shown below (Figure 17), and this particular series has had enough time to clearly show signs of growth. The number of dilutions must be sufficient to reach a point where no organisms are transferred to the next subsequent dilution. Ideally, there will be at least two or more dilutions where no growth will appear, or the resulting MPN is less likely to be accurate, if at all usable.

Once the dilution series has been created, generally carried out to eleven dilutions for the biomachining tests, part of that series is used to inoculate the tubes used as growth indicators in the most probable number test. In a three-tube MPN, an array of test tubes containing 9 mL of sterile media is set up consisting of an arbitrary number of columns of three test tubes each. In the biomachining experiment, one column was set up for each dilution from 10^{-4} to 10^{-11}, resulting in a 3 X 8 array, or a total of 24 test tubes (Figure 18). Each tube in a given column receives 1 mL from its designated dilution, resulting in three 10 mL solutions. Once all 24 tubes have been inoculated from their designated dilutions, the tube array is incubated until signs of growth appear. Once enough time has passed to ensure all the tubes that will show growth have, the array is removed from incubation. Each three-tube column is given a score corresponding to how many of the tubes show growth, ranging from +0 for no growth in any tube to +3 for all tubes showing growth. For the statistical analysis, the first column where no growth (+0) occurs is noted. The sequence of scores of this column and the two preceding it, such as +3 +2 +0, is used to find a numerical value in tabulated MPN tables. This numerical value is then multiplied by the inverse of the dilution power of the middle column. As an example, if the sequence of scores is +3 +2 +0 centered on the 10^{-8} dilution, then the value corresponding to a sequence of +3 +2 +0 in the table (say, 9.3) is multiplied by 10^{8}, resulting in a total approximate bacterial concentration of the original sample of $9.3*10^{8}$ organisms/mL.

A typical dilution series is shown below in Figure 17, and a three-tube MPN is shown in Figure 18. The MPN technique was repeated for each experiment, both in the starting solution and at the end of each time period for each jar.

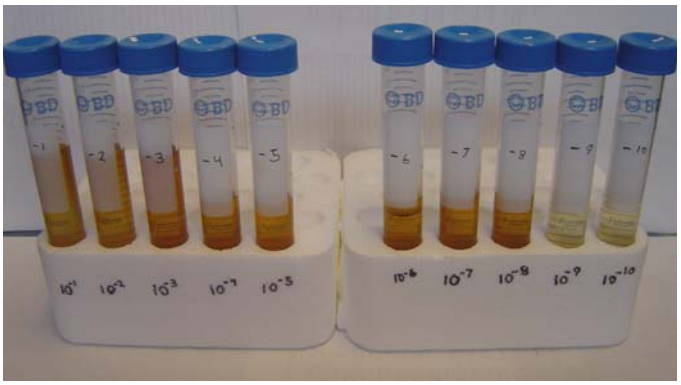

Figure 17: A Typical Dilution Series (note: growth stops at the 9th dilution)

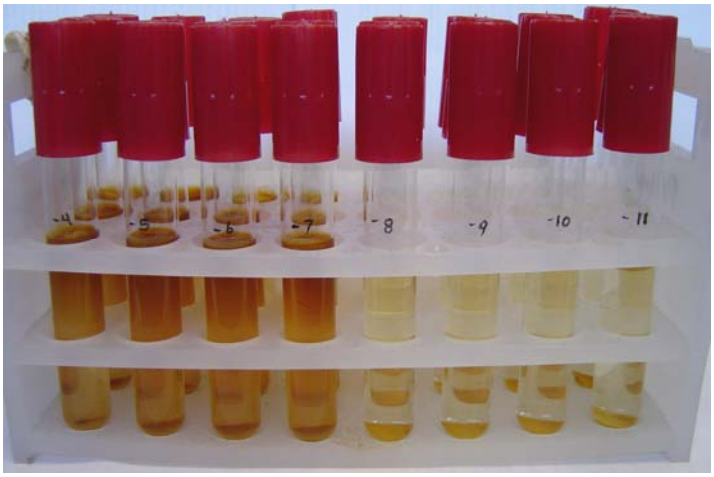

Figure 18: Typical 3-Tube MPN (note: growth stops at 8th dilution)

4.5. Sample Preparation

For the main experiment, first samples of 99.99% pure copper (Alloy 101) were prepared from plate stock. The copper was cut into roughly uniform cubes of approximately 12-15 mm to a side using a wire EDM process. One face was then chosen and ground to the desired level of surface finish. Polishing of the chosen side was carried out using grinding wheels fitted with paper containing Si-C of various grit sizes. The grit sizes chosen were 320, 600, and 1200, each used in sequence until the desired finish level was reached. For the highest level of surface finish, a fabric wheel covered with a .6µm diamond particle slurry was used. Once polished, every sample was contained in a sealed plastic bag to reduce surface oxidation before use in the experiment. A total of sixteen samples were prepared and used. Four were made for each level of surface finish: control and experimental pieces for 24 hour exposure, and control and experimental pieces for 48 hour exposure.

Before use in the experiments, each sample was subjected to roughness measurement using a profilometer. On the chosen polished side of each sample, three tests were done along one direction, and three were done in a perpendicular direction. In this measurement, only the Ra value of roughness was used, and the and the specific profilometer settings were: data length: 5.6 mm, cutoffs: 7, Gaussian filter, Ls: .008 mm, and Lc: .8 mm. To obtain an estimate of overall surface roughness, the average of all six readings was used.

Finally, each sample was viewed using a SEM. Pictures were captured at 100X and 500X. Due to the similarities of surfaces of identical finish, only representative micrographs are included for the pre-experiment portion of the data.

4.6. Aseptic Technique

Before each experiment, every container and sample was sterilized to avoid potential contamination. The sealed jars used were autoclaved and were only opened under a bacterial culture hood, shown below in Figure 19. The copper samples and the plastic mounts that held them upright were sterilized chemically by soaking them in

100% ethanol for 1-2 minutes. They were then air-dried on a sterile metal surface under the culture hood that had also been sterilized with 100% ethanol.

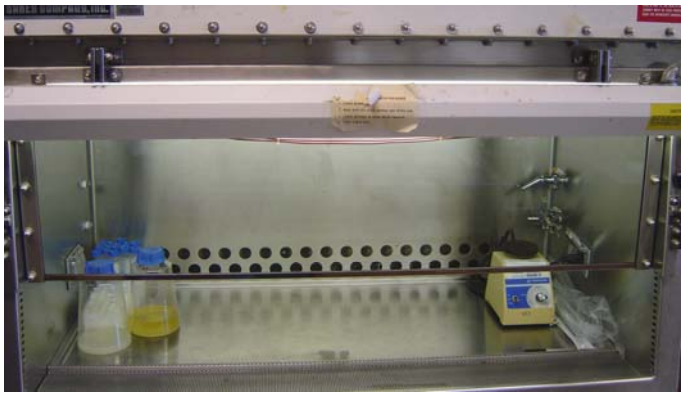

Figure 19: Microbial Laminar-Flow Hood Used in the Experiments

All media and bacterial samples were transferred between containers using sterile, sealed pipettes and a pipettor that was cleaned with 100% ethanol. Gloves were always worn and were also rinsed with ethanol. Finally, the working surface inside the hood was also wiped down with 100%alchohol.

4.7. Beginning an Experiment

For an experimental run using bacteria, four sterile flasks were filled with 150mL of fresh 9K media and inoculated with 2mL each from an existing batch culture under the bacterial culture hood. The flasks, with vented tops replaced, were then shaken at 120 RPM and incubated at 35°C for 48 hours. Each flask was then opened in the hood and poured into a 1L sterile flask and mixed. Before pouring the mixed bacterial solution into the test jars, a sample was taken for an estimate of the initial bacterial concentration using a 3-tube MPN.

Each jar was next opened and filled with approximately 150 mL of the mixed bacterial broth. In the case of the control tests, each jar was filled with 150 mL of fresh 9K media. After each metal sample designated for the particular test (one of each finish) and corresponding plastic mount finished air-drying from sterilization with ethanol, they were gently placed on the bottom of the jars with the polished metal surface facing upward. A typical jar with plastic sample mount is shown below in Figure 20.

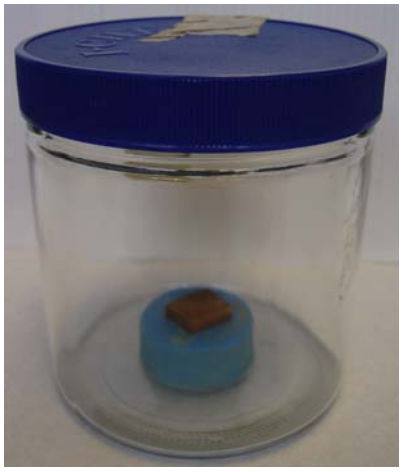

Figure 20: Experiment Jar with Sample in Mount (without media)

Each jar was then sealed and placed in an incubator again at 35°C without shaking for the designated time period. Four such experimental runs were conducted: control/with bacteria for 24 hours and control/with bacteria for 48 hours.

4.8. Finishing an Experiment

At the completion of each time period, the jars were removed from the incubator and the samples were removed. Each sample was then rinsed gently with de-ionized water and air-dried, which was finished by blotting with lint-free wiping paper. For transfer to the roughness testing, each was wrapped in lint-free wipes and stuffed into a conical tube.

The remaining bacterial broth in each jar was sampled for final MPN's, resulting in a total of five for each experimental run. Just as before, 1 mL (this time from each jar) was put into 9 mL of sterile 9K media, and the dilutions were carried out eleven times. Tubes 6-11 were then used in each three-tube MPN to estimate bacterial concentrations.

Just as before the experiments, roughness values were taken on the finished face of the cubical sample. Again, three values were taken in one direction, and three were taken perpendicular to that. The average of the six Ra values is used in the experimental results presented below. SEM micrographs were also again taken of each surface, at 100X and 500X magnification, for comparison with the surfaces before exposure. An exception to this is the included micrograph at higher magnification believed to show bacterial traces, but this is elaborated upon below.

4.9. Material Removal Rate

A final experiment was conducted in an attempt to obtain a crude estimate of the material removal rate of the bacteria, a necessary quantity in any machining process. Previous work gave some values for this parameter, and it was desired to see if current experiments produced comparable numbers, as well as determine if it changes with time. For this test, a pre-experiment culturing and MPN were carried out as detailed above in *4.1* and *4.7*. Four copper foil sheets were cut from shim stock of 0.001 in. thick Cu Alloy 110 in a designated size of 4 mm by 6 mm, and their masses were measured.

This material is slightly different from the very pure plate stock used in the roughness tests (the foil having a purity of only 99.9% Cu), but it was deemed similar enough to be relevant and was the only available variety of copper that came in such a thin foil. After cutting, and then sterilizing in ethyl alcohol, two pieces of foil were then fully submerged in 150 mL of bacterial broth and the other two were submerged in equal quantities of sterile 9K media. All tests were conducted in the same sample jars used in the roughness experiments, which were sealed and incubated at 35° C for the specified length of time (24 or 48 hours). At the conclusion of the time period, each piece of foil was removed, rinsed with de-ionized water, and air dried. The final masses were recorded and then compared to the initial. Using the mass difference and time period, as well as the known density value for the specific copper alloy[27], a material removal rate was then calculated for each piece of foil, which was assumed to be constant over the given time period.

Chapter 5. Experimental Data

5.1. Roughness Results Summary

The results of the experiment described above are summarized in Figure 22 below. Every sample exposed to the bacteria experienced a drastic increase in overall roughness, well beyond any bounds of error in the profilometer. The controls, by contrast, all showed little or no increase in roughness. The slight variations in the control roughness values could be attributed to the acidic nature of the media (pH of ~2.5), as well as measurement error in the profilometer. It was observed that after exposure to even sterile media, individual grains and boundaries became clearly visible, indicating at least some corrosion on the surface.

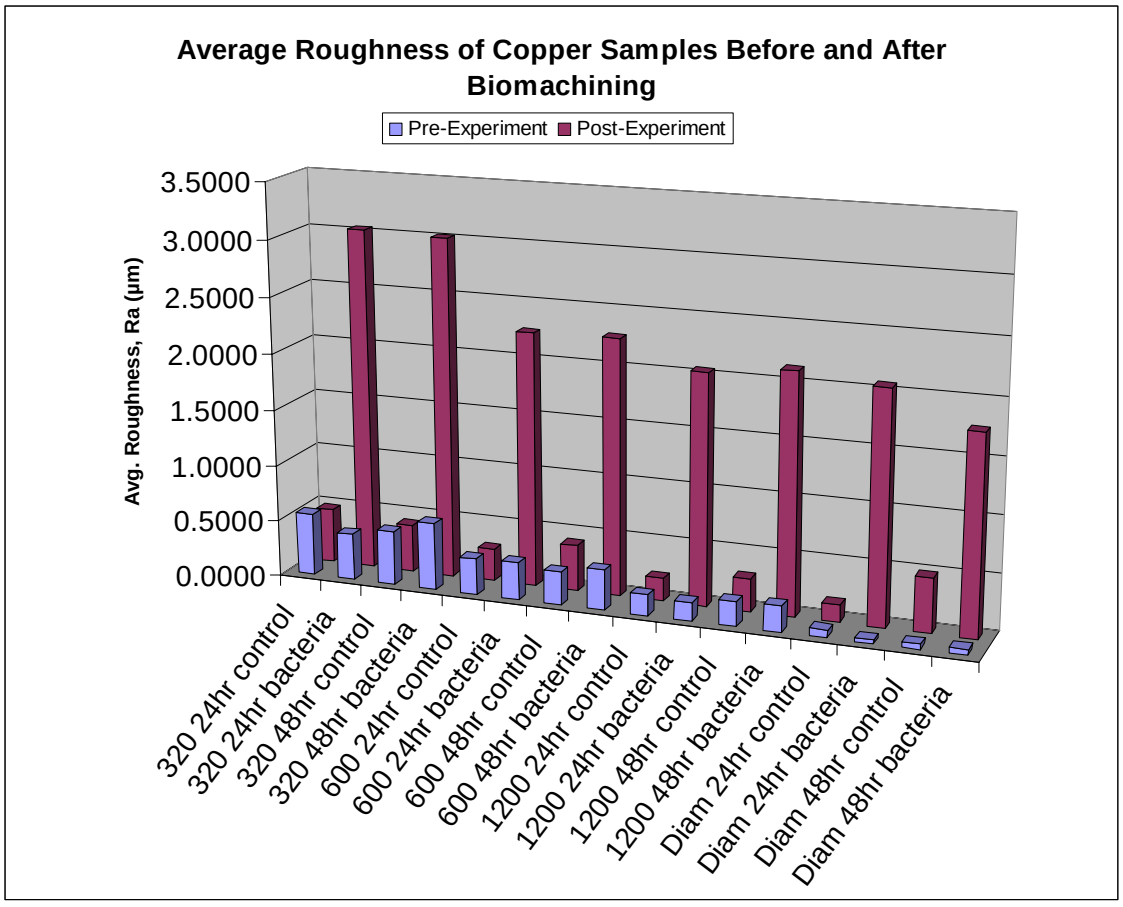

Figure 21: Summarized Experimental Results

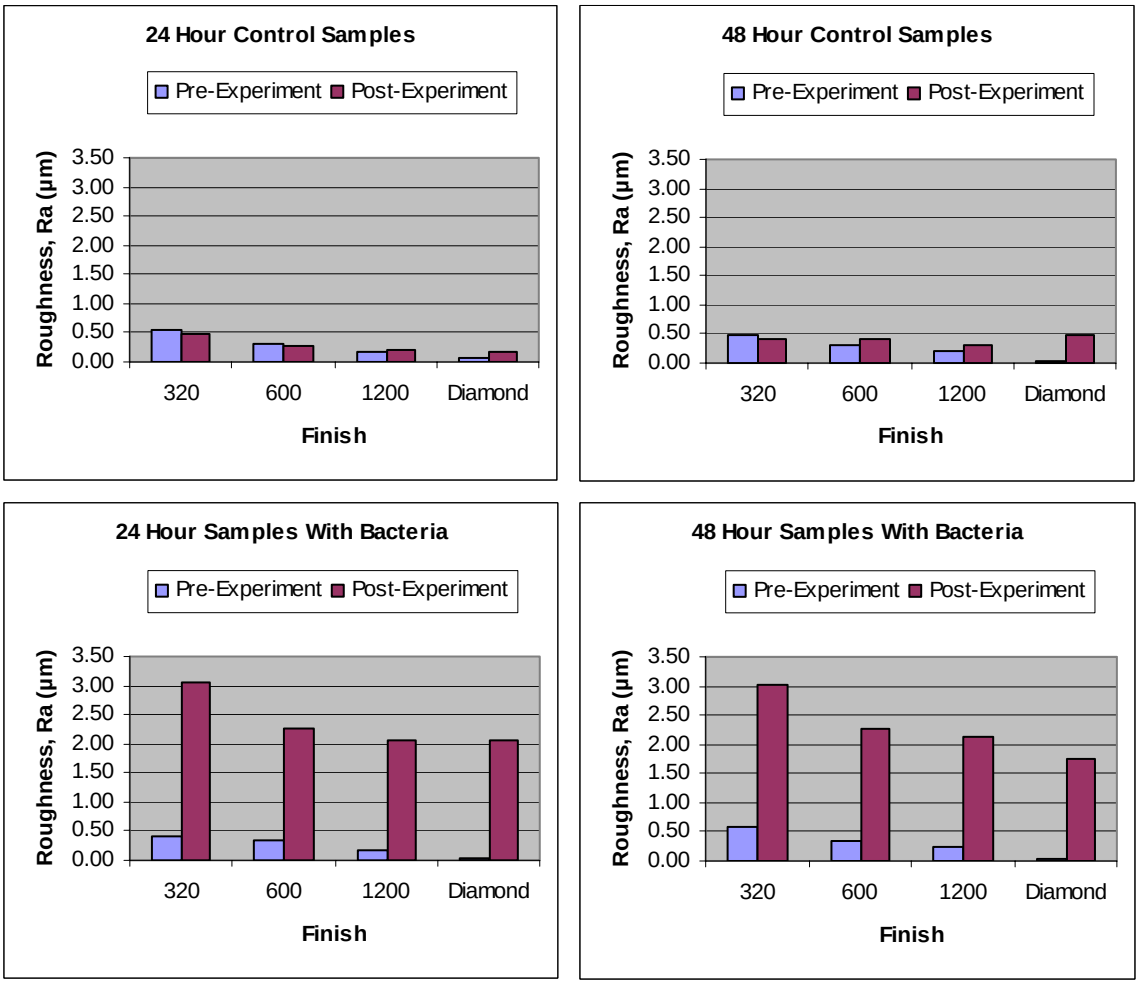

Figure 22: Summary of Roughness Values Before and After Incubation for Control Samples (top) and Samples Incubated with Bacteria (bottom)

The bacterial populations showed little change in growth behavior beyond regular replication, although some (the 1200 and Diamond for 48 hours) did show some decrease. The variations in these numbers have many possible sources of error, including the inaccuracies inherent in the MPN estimation process, possible breakdowns in aseptic technique, uneven mixing at each dilution, and even slight errors in the amounts of solution transferred between tubes.

5.2. Bacterial Concentrations

5.2.1. Initial Bacterial Concentrations

24 Hours:

The MPN series ended in a sequence of +3 +3 +0 (i.e., for two dilutions, all three tubes showed growth, and then the next higher series had no tubes showing growth) centered at the 10^{-7} dilution. This corresponds to an approximate concentration of $2.4*10^{7}$ organisms/mL.

48 hours:

The MPN series resulted in a sequence of +3 +1 +0, centered at the 10^{8} dilution. This corresponds to an approximate concentration of $4.3*10^{7}$ organisms/mL.

5.2.2. Final Bacterial Concentrations

24 hours:

320	MPN series of +3 +1 +0 centered at the 10^{-8} dilution, bacterial concentration of $4.3*10^{7}$ organisms/mL.
600	MPN series of +3 +3 +0 centered at the 10^{-7} dilution, bacterial concentration of $2.4*10^{7}$ organisms/mL.
1200	MPN series of +3 +3 +0 centered at the 10^{-7} dilution, bacterial concentration of $2.4*10^{7}$ organisms/mL.
Diamond	MPN series of +3 +3 +1 centered at the 10^{-8} dilution, bacterial concentration of $4.3*10^{7}$ organisms/mL.

48 hours:

320	MPN series of +3 +2 +0 centered at the 10^{-8} dilution, bacterial concentration of $9.3*10^{7}$ organisms/mL.
600	MPN series of +3 +1 +0 centered at the 10^{-8} dilution, bacterial concentration of $4.3*10^{7}$ organisms/mL.
1200	MPN series of +3 +3 +0 centered at the 10^{-7} dilution, bacterial concentration of $2.4*10^{7}$ organisms/mL.
Diamond	MPN series of +3 +3 +0 centered at the 10^{-7} dilution, bacterial concentration of $2.4*10^{7}$ organisms/mL.

5.3. SEM Pictures

The qualitative results gleaned from the SEM pictures of each surface, all of which are included in Appendix B, reinforce the drastic changes shown in the numerical data between pre and post-exposure to *A. ferrooxidans.* Before exposure to either media or bacteria, each surface shows rather predictable, regular patterns for each level of finish. As expected, the lowest value of surface finish (the 320 grit paper) gives the surface a rather jagged appearance with large canyons carved in parallel by the rather large particles as they removed the surface material. Edges of these trenches can be seen to have many irregular portions along their length, with almost complete detachment of

some of the larger chunks of material. As the surface finish become finer, the carved trenches become narrower and much more regular, until we reach the .6 µm diamond level where hardly any surface features can be seen.

The post-experiment SEM micrographs show the drastic contrast between the control surfaces, which only experienced the acidic media, and those exposed to the bacteria.

Each surface exposed to the bacteria reveals an extremely uneven surface, marked by numerous depressions and craters. On some of the more level sections, highly ordered angular plates can be seen. The higher level surfaces vary from relatively smooth to an almost pin-cushion-like appearance. The control surfaces show slight changes in the depths of the aforementioned trenches, but the patterns are still very regular and don't seem to change very much from before the experiment.

It is apparent in some of the control SEM micrographs that grain boundaries are visible. The corrosive 9K media apparently preferentially attacks the less organized amorphous regions in between the individual grains of copper, so this may explain some of the roughness changes seen in the control samples.

On some of the higher magnification micrographs for samples incubated with bacteria, especially the 600 finish sample incubated for 48 hours, small regular rod shapes can be seen on some of the lower level surfaces. It his highly unlikely that these actually are individuals of *A. ferrooxidans*, but the general shape and size suggest that they may be remnants of where the bacteria once adhered to the surface. Corrosion caused by single individuals may have created depressions that show up in these images. Actual bacteria would most likely have been vaporized by charge buildup from the electron source of the microscope. A picture at 2500X magnification of the 600 finish sample with the possible bacterial remnants is shown below in Figure 23.

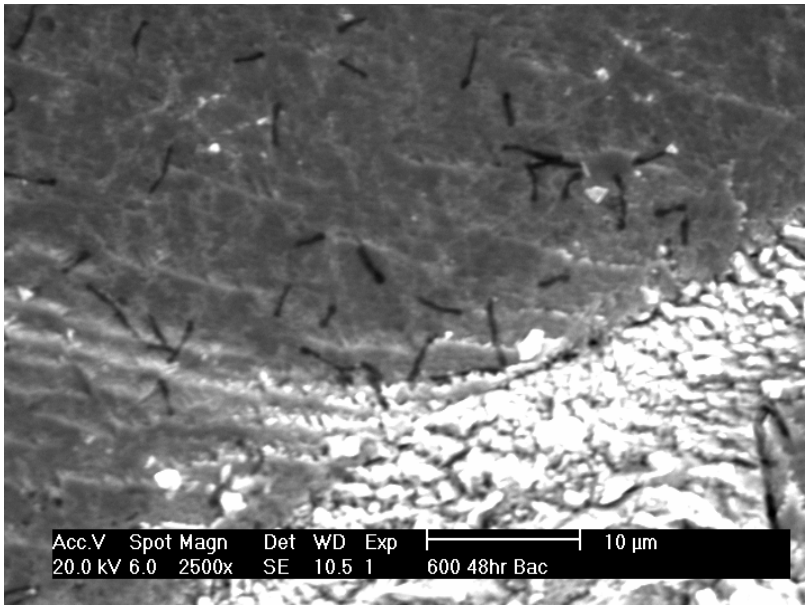

Figure 23: Possible Bacterial Traces on a Copper Surface

5.4. Material Removal Rate

The copper foil pieces displayed drastic differences in mass after exposure to bacterial solutions of *A. ferrooxidans*, indicating a pronounced removal of material. The control experiments, while displaying some material loss due to the acidic nature of the 9K media, have an almost insignificant change in mass when compared to the pieces exposed to the bacteria. The results are summarized below in Table 6. The MPN resulted in +3 +1 +0 centered at the 10^{-8} dilution, corresponding to initial bacterial concentrations of $4.3*10^{7}$ organisms/mL for both bacterial tests..

Table 6: Material Removal Rate Data

Foil Label	Initial Mass	Final Mass	Material Removal Rate
24 hr Control	0.5295 g	0.5250 g	$8.738*10^{-4}$ mm/hr
24 hr Bacteria	0.5330 g	0.3691 g	0.032 mm/hr
48 hr Control	0.5250 g	0.5245 g	$4.855*10^{-5}$ mm/hr
48 hr Bacteria	0.5259 g	0.3512 g	0.017 mm/hr

Aside from the large mass differences exhibited by the foil pieces exposed to the bacteria, visible physical differences were also observed between them and the control pieces. The pieces exposed to bacteria had visible grain boundaries and were much less lustrous than their control counterparts.

6. Conclusions

The most obvious conclusion that can be made using the experimental results is that the "machining" effect on copper produced by *Acidithiobacillus ferrooxidans* is very detrimental to surface finish. This largely uneven corrosion seems to be produced regardless of initial finish, at least past the rather rough 320 grit size. In this current setup, bacterial machining is impractical for fine control of nano-scale material removal. That being said, the process could still have potential if some possible refinements are added.

The rather uneven nature of the corrosion effect could be partially caused by the deposition of the solid waste products of the copper corrosion on the sample surface. This material could effect how well the bacteria adhere to the copper surface, thus shielding a covered area from bacterial corrosion. One fairly simple remedy for this is to conduct the experiment in a non-quiescent fluid environment. If a properly controlled flow of media is constantly forced over the sample, it may carry away the waste material, thus leaving unaffected material exposed for bacterial adhesion. The optimal flow rate would promote waste removal while not preventing the bacteria's access to the surface, and this would have to be determined through further empirical testing.

A slightly more complex modification of this process would involve the use of single-crystal copper. The irregular pattern of crystal grains, and the disorganized nature of the grain boundaries may contribute to the lack of evenness in the corrosion. Single grain copper crystals could potentially eliminate effects of etching at the grain boundaries by the 9K media, thus exposing a relatively smooth surface to the bacteria. If this is combined with forced fluid flow over the sample, much more uniformity in material removal could potentially be achieved.

The material removal rate tests were very simple in nature, but they still suggest possible trends in the removal behavior exhibited by the bacteria. The noticeably lower material removal rate for the 48 hour time period suggests that not only is the removal rate not uniform, but it slows down with time. The otherwise identical 24 hour test suggests an initially high MRR, which may slow down due to waste buildup in the liquid media or lack of oxygen. The first suggested cause seems more likely, especially since the media used in the test exhibited a much deeper orange color, as did the precipitate, than the typical liquid media exhibiting growth. The color suggests a buildup of copper compounds, most likely CuS, as suggested in the reaction diagrams in *2.3*. One possible way to make the material removal rate more uniform with time is to constantly supply fresh, aerated media to and flush waste compounds from the whole working fluid environment.

Future work could thus initially include a combination of the three modifications suggested above. A single crystal of copper would be able to present the most even surface possible to the bacteria, as no grain boundaries would exist to be corroded by the media. If fresh media were constantly supplied and forced over the surface of the workpiece at a controlled flow rate, waste compounds could be removed as they are generated, and the copper surface could remain evenly exposed for bacterial machining. After these initial modifications, other process and environment parameters can be varied to further refine and find the limits of biomachining.

References

[1] Williams, K. and Gupta, K. and Wasilik, M. (2003) "Etch Rates for Micromachining Processing-Part II." Journal of Microelectromechanical Systems, Vol. 12, No. 6, pp. 761-778.

[2] Uno, Y., Kaneeda, T. and Yokomizo, S. (1993) "Fundamental study on biomachining (machining of metals by Thiobacillus ferrooxidans)." Transactions of the Japan Society of Mechanical Engineers, Part C, Vol. 59, pp. 3199-3204.

[3] Kumada, M., Kawakado, T., Kobuchi, S., Uno, Y., Maeda, S. and Miyuki, H. (2001) "Investigations of fine biomachining of metals by using microbially influenced corrosion - Differences between steel and copper in metal biomachining by using Thiobacillus Ferrooxidans." Zairyo to Kankyo/ Corrosion Engineering, Vol. 50, pp. 411-417.

[4] Kurosaki, Y., Matsui, M., Nakamura, Y., Murai, K. and Kimura, T. (2003) "Material processing using microorganisms (An investigation of microbial action on metals)." JSME International Journal, Series C: Mechanical Systems, Machine Elements and Manufacturing, Vol. 46, pp. 322-330.

[5] Uno, Y., Kaneeda, T. and Yokomizo, S. (1996a) "Fundamental study on biomachining (machining of metals by Thiobacillus ferrooxidans)." JSME International Journal, Series C, Vol. 39, pp. 837-842.

[6] Uno, Y. Kaneeda, T., Yokomizo, S. and Yoshimura, T. (1996b) "Fundamental study on electric field assisted biomachining," Journal of the Japan Society for Precision Engineering, Vol. 62, pp. 540-543.

[7] Zhang, D. and Li, Y. (1996) "Possibility of biological micromachining used for metal removal," Science in China Series C Life Sciences, Vol. 41, pp. 151-156.

[8] Zhang, D. and Li, Y. (1998), "Studies on kinetics and thermodynamics of biomachining pure copper." Science in China Series C Life Sciences, Vol. 42, pp. 57-62.

[9] Gomez, C., Blazquez, M. and Ballester, A. (1999) "Bioleaching of a Spanish complex sulphide ore bulk concentrate." Minerals Engineering, Vol. 12, pp. 93-106.

[10] Konishi, Y., Kubo, H. and Asai, S. (1992) "Bioleaching of zinc sulfide concentrate by Thiobacillus ferrooxidans," Biotechnology and Bioengineering, Vol. 39, pp.66-74.

[11] Olson, G. (1991) "Rate of pyrite bioleaching by Thiobacillus ferrooxidans: Results of an interlaboratory comparison." Applied Environmental Microbiology, Vol. 57 (3), pp. 642–644.

[12] Bond, D., Holmes D., Tender L. and Lovley D. (2002) "Electrode-reducing microorganisms that harvest energy from marine sediments," Science. 295:483-5.

[13] Lovley, D. R., Phillips, E. J. P., Gorby, Y. A., Landa, E. R. (1991) "Microbial reduction of uranium," Nature, Vol. 350, pp. 413-416.

[14] Lovley, D. R. (2003) "Cleaning up with genomics: applying molecular biology to bioremediation." Nature Reviews, Vol. 1, pp. 35-44.

[15] Viamajala, S., Peyton, B., and Petersen, J. (2003) "Modeling chromate reduction in *Shewanella oneidensis* MR-1: development of a novel dual-enzyme kinetic model," Biotechnology and Bioengineering, Vol. 83, No. 7, pp. 790-797.
[16] Dinh, H., Kuever J., Mussmann M., Hassel A., Stratmann M. and Widdel F. (2004) "Iron corrosion by novel anaerobic microorganisms." Nature, Vol. 427(6977), pp. 829-832.
[17] Chaudhuri, S., and Lovley, D. (2003) "Electricity generation by direct oxidation of glucose in mediatorless microbial fuel cells." Nature Biotechnology, Vol. 21, No. 10, pp. 1229-1232.
[18] Levett, Paul N. Anaerobic Bacteria: A Functional Biology. Open University Press; Philadelphia: 1990.
[19] Wilkinson, J. F. Introduction to Microbiology. John Wiley and Sons; New York: 1975.
[20] MVTechnologies, Inc. (MVTI)
[21] Walsh, E. O'F. An Introduction to Biochemistry. English Universities Press; London: 1961.
[22] Zehnder, A. J. B. Biology of Anaerobic Microorganisms. John Wiley and Sons; New York: 1988.
[23] http://www.vkm.ru/catalog/pdf/media.pdf
[24] Johnson, Macvicar, and Rolfe. "A New Solid Medium for the Isolation and Enumeration of Thiobacillus Ferrooxidans and Acidophilic Heterotrophic Bacteria." The Journal of Microbiological Methods. Vol. 7, Number 1, 1987. pp. 9-18.
[25] Southam, G. and Beveridge, T. J. "Enumeration of Thiobacilli within pH-Neutral and Acidic Mine Tailings and Their Role in the Development of Secondary Mineral Soil." Applied and Environmental Microbiology. Vol. 58, Number 6, June 1992. pp. 1904-1912.
[26] http://www.jlindquist.net/generalmicro/102dil3.html
[27] http://www.suppliersonline.com/propertypages/C11000.asp

Appendix A: Experimental Roughness Values

A.1 Pre-Experiment

Label	Ra Values (µm)	Average (µm)
320 24hr control	0.6168	0.5536
	0.5284	
	0.5091	
	0.4927	
	0.5757	
	0.5987	
320 24hr bacteria	0.3703	0.4132
	0.3811	
	0.3513	
	0.3633	
	0.5117	
	0.5014	
320 48hr control	0.4765	0.4834
	0.5057	
	0.5501	
	0.4471	
	0.4231	
	0.4979	
320 48hr bacteria	0.6029	0.5958
	0.5349	
	0.5426	
	0.7305	
	0.6431	
	0.5206	
600 24hr control	0.301	0.3215
	0.3016	
	0.2771	
	0.3918	
	0.2947	
	0.3628	
600 24hr bacteria	0.3074	0.3319
	0.317	
	0.363	
	0.3431	
	0.3239	
	0.3368	
600 48hr control	0.2778	0.2967
	0.2859	

	0.2534	
	0.3205	
	0.3024	
	0.3399	
600 48hr bacteria	0.3735	0.3596
	0.3866	
	0.3364	
	0.3568	
	0.3388	
	0.3657	
1200 24hr control	0.1555	0.1842
	0.1719	
	0.1693	
	0.2184	
	0.1963	
	0.1939	
1200 24hr bacteria	0.1979	0.1644
	0.1654	
	0.1797	
	0.1432	
	0.145	
	0.1549	
1200 48hr control	0.2055	0.2212
	0.2008	
	0.2166	
	0.2377	
	0.2449	
	0.2217	
1200 48hr bacteria	0.2699	0.2306
	0.2583	
	0.2232	
	0.2181	
	0.2195	
	0.1946	
Diam 24hr control	0.0633	0.0690
	0.0783	
	0.0745	
	0.0566	
	0.0744	
	0.0666	
Diam 24hr bacteria	0.0304	0.0346
	0.0382	
	0.0369	

	0.0295	
	0.0399	
	0.0328	
Diam 48hr control	0.0504	0.0487
	0.0519	
	0.0476	
	0.0477	
	0.0506	
	0.0437	
Diam 48hr bacteria	0.04	0.0502
	0.0383	
	0.0368	
	0.0548	
	0.046	
	0.0853	

A.2 Post-Experiment

Label	Ra Values (µm)	Average (µm)
320 24hr control	0.5093	0.4806
	0.4717	
	0.4466	
	0.5079	
	0.4779	
	0.4704	
320 24hr bacteria	4.0345	3.0396
	4.1263	
	2.2224	
	1.1939	
	3.4905	
	3.1699	
320 48hr control	0.4159	0.4162
	0.4018	
	0.3825	
	0.4539	
	0.4349	
	0.4082	
320 48hr bacteria	2.6231	3.0146
	2.9079	
	3.6229	
	2.9167	
	3.0213	
	2.9954	
600 24hr control	0.2934	0.2847
	0.2661	

	0.3096	
	0.2788	
	0.2757	
	0.2846	
600 24hr bacteria	2.816	2.2547
	2.1324	
	2.1519	
	2.1726	
	2.1195	
	2.1358	
600 48hr control	0.4503	0.4087
	0.3814	
	0.3961	
	0.394	
	0.4267	
	0.4037	
600 48hr bacteria	2.0805	2.2723
	1.8524	
	2.4643	
	1.8637	
	2.4745	
	2.8985	
1200 24hr control	0.2211	0.2039
	0.2032	
	0.2108	
	0.2235	
	0.1855	
	0.1792	
1200 24hr bacteria	2.5051	2.0462
	2.3025	
	1.9845	
	1.5742	
	1.7522	
	2.1588	
1200 48hr control	0.3195	0.2935
	0.2736	
	0.2983	
	0.3315	
	0.2681	
	0.27	
1200 48hr bacteria	2.3707	2.1281
	2.0559	
	1.9257	

	2.3222	
	2.0152	
	2.079	
Diam 24hr control	0.1773	0.1588
	0.1811	
	0.1661	
	0.1425	
	0.1438	
	0.142	
Diam 24hr bacteria	1.9187	2.0563
	2.0323	
	2.2641	
	2.3499	
	1.9352	
	1.8374	
Diam 48hr control	0.4644	0.4828
	0.5018	
	0.4834	
	0.4961	
	0.5621	
	0.3888	
Diam 48hr bacteria	2.0618	1.7603
	1.2904	
	1.3919	
	1.7156	
	1.8022	
	2.2998	

Appendix B: SEM Micrographs

B.1. Pre-Experiment SEM Micrographs

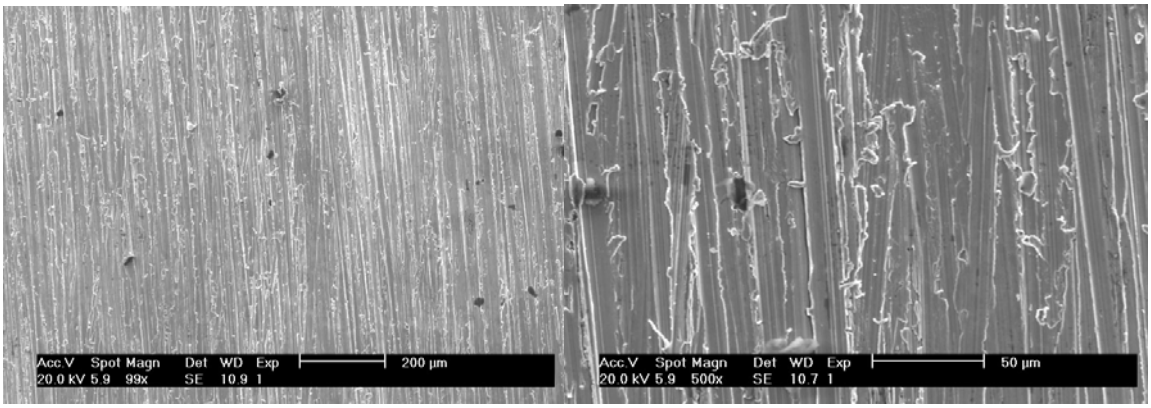

Typical 320 Finish (images from 24 Hour Control)

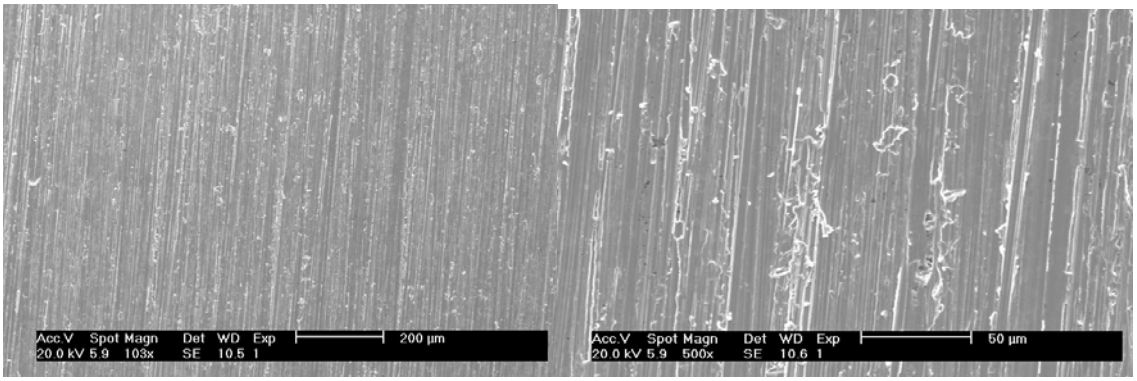

Typical 600 Finish (images from 24 Hour Control)

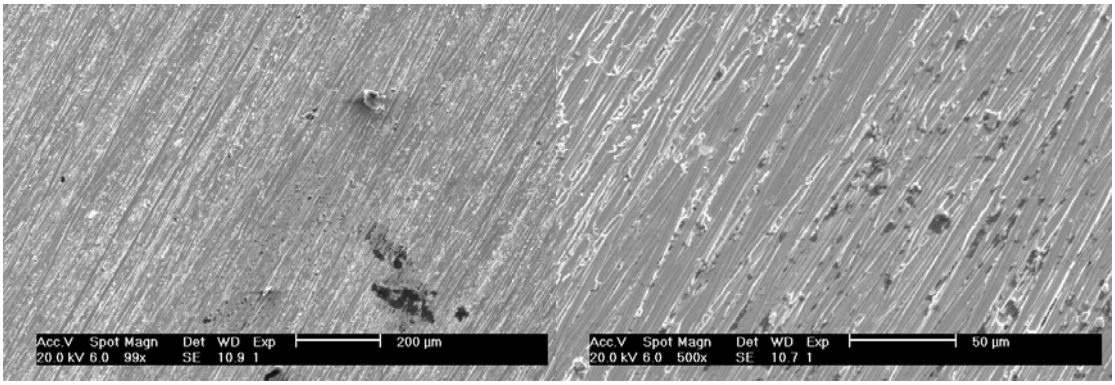

Typical 1200 Finish (images from 48 Hour Control)

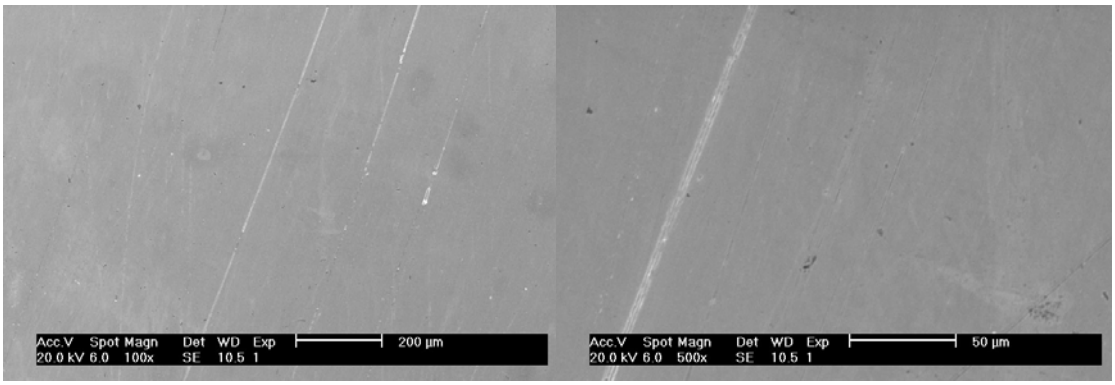

Typical Diamond Finish (images from 48 Hour Control)

B.2. Post-Experiment SEM Micrographs

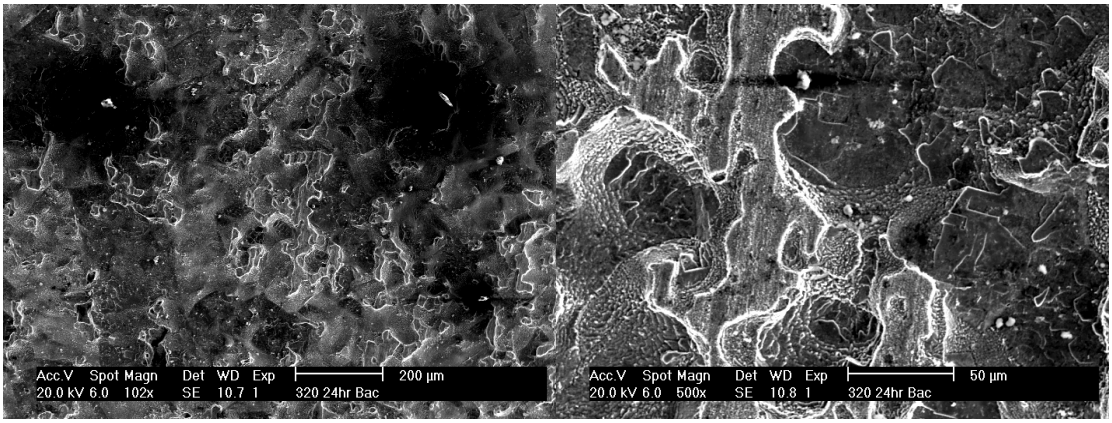

320 Finish, 24 Hour, With Bacteria

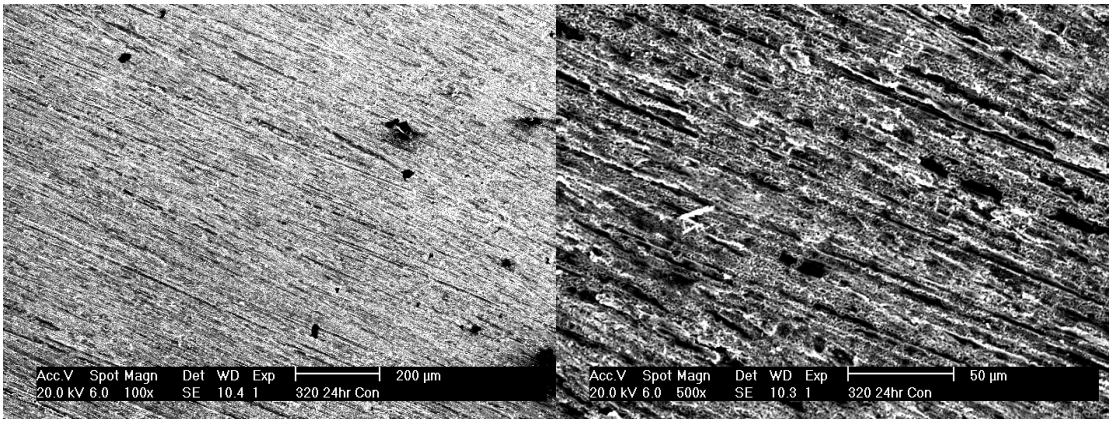

320 Finish, 24 Hour, Control

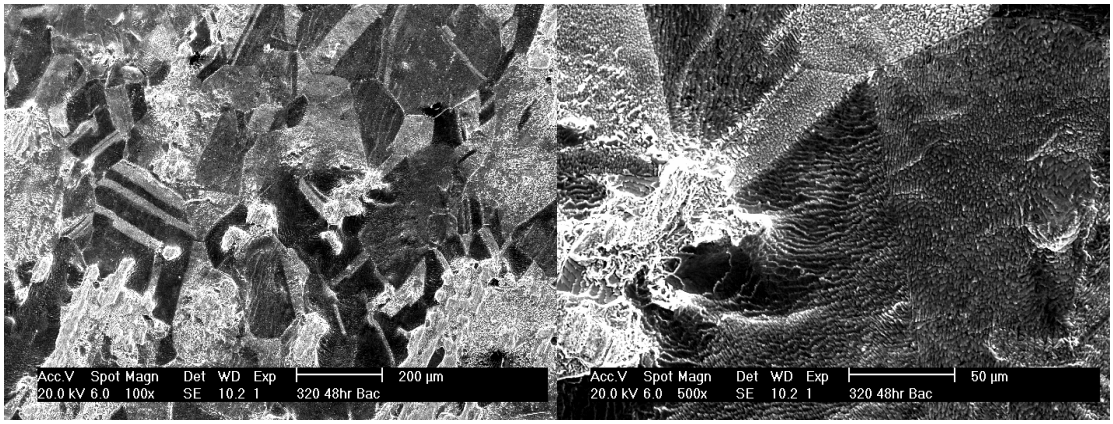

320 Finish, 48 Hour, With Bacteria

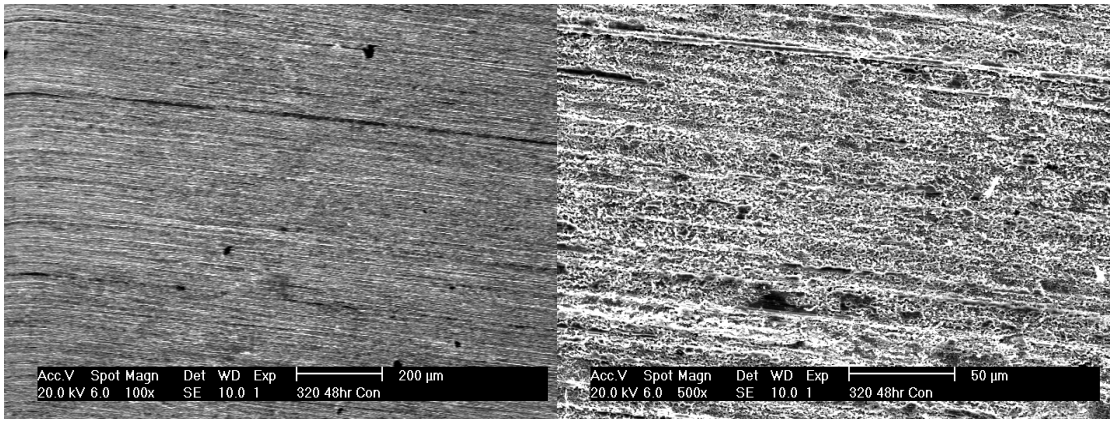

320 Finish, 48 Hour, Control

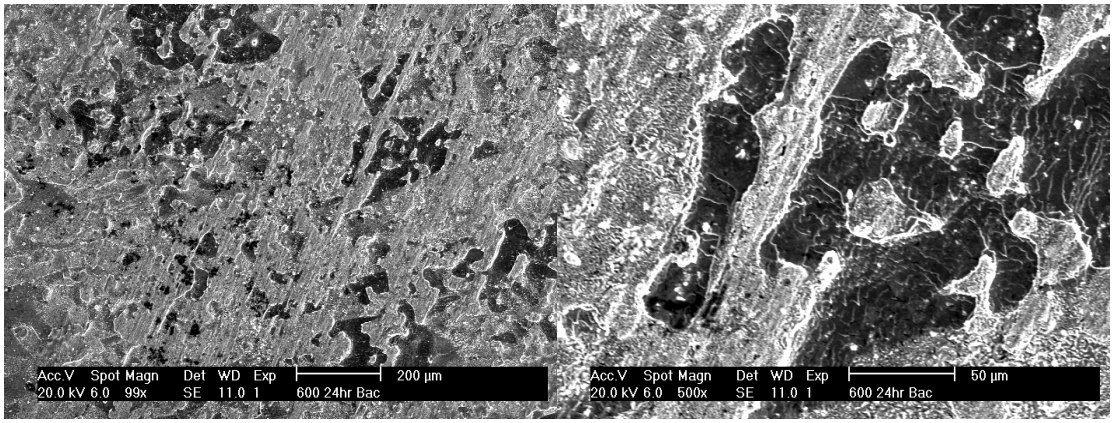

600 Finish, 24 Hour, With Bacteria

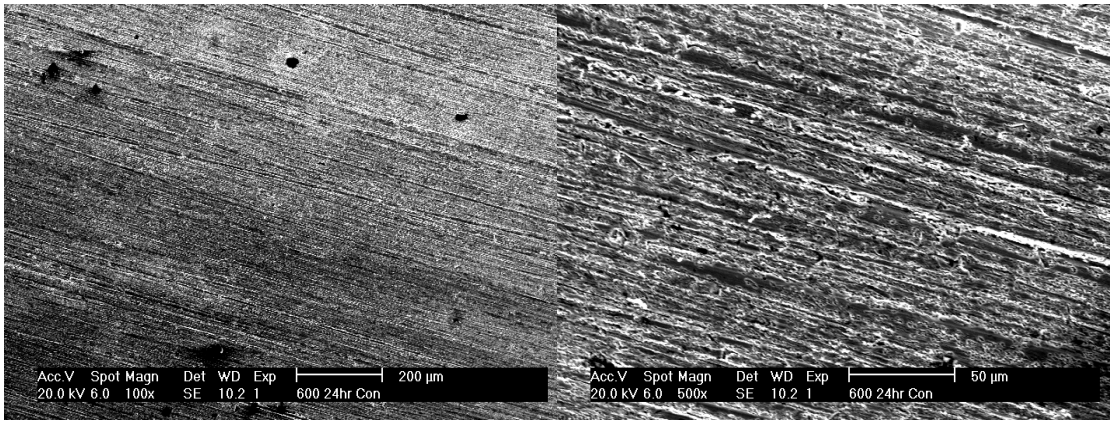

600 Finish, 24 Hour, Control

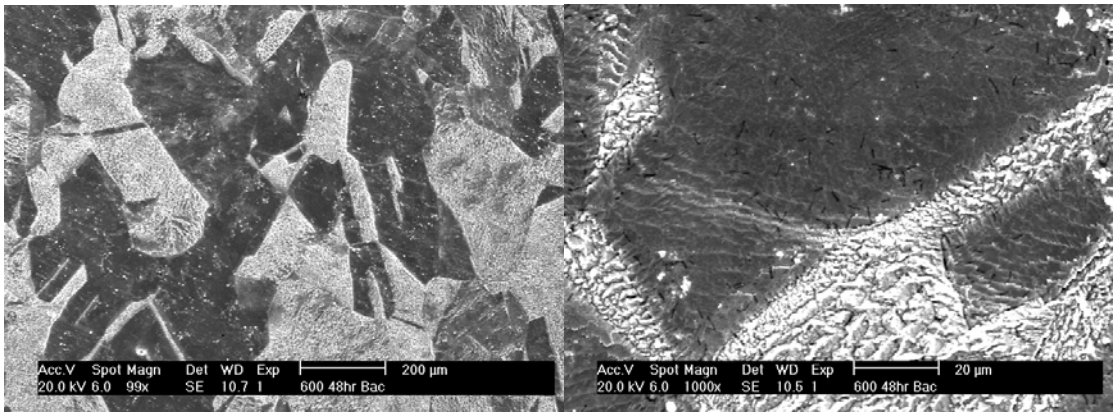

600 Finish, 48 Hour, With Bacteria

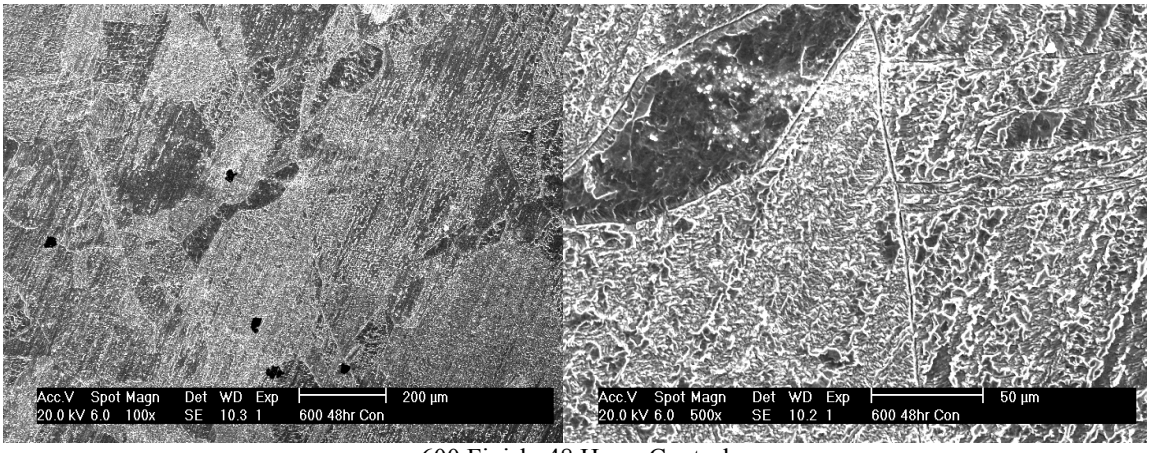

600 Finish, 48 Hour, Control

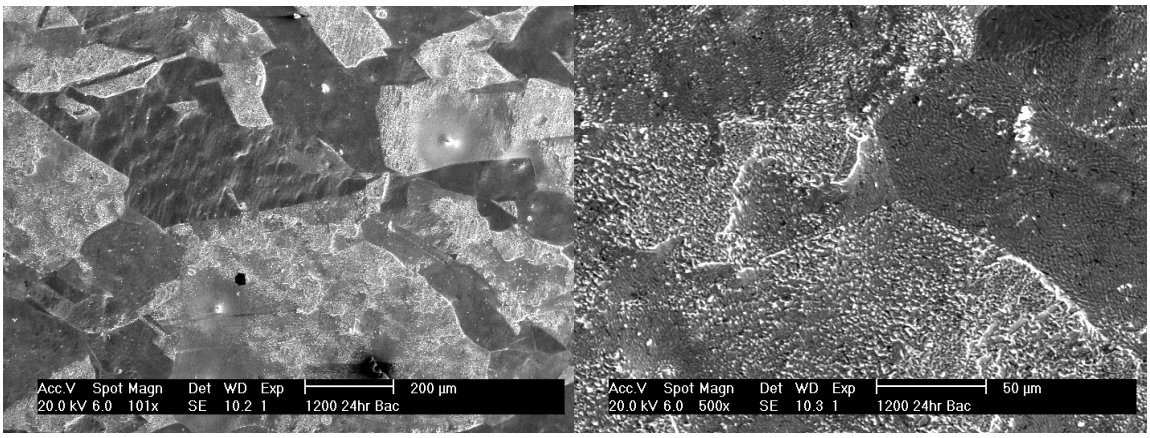

1200 Finish, 24 Hour, With Bacteria

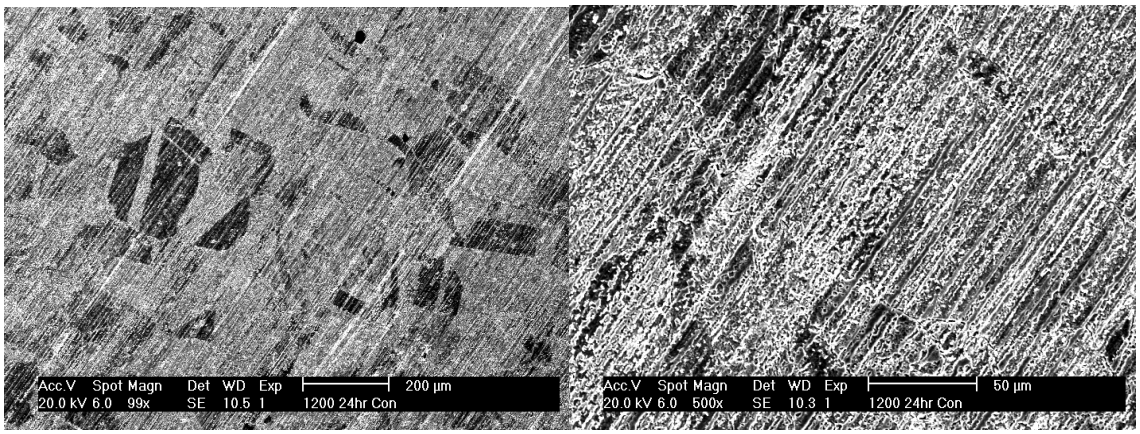

1200 Finish, 24 Hour, Control

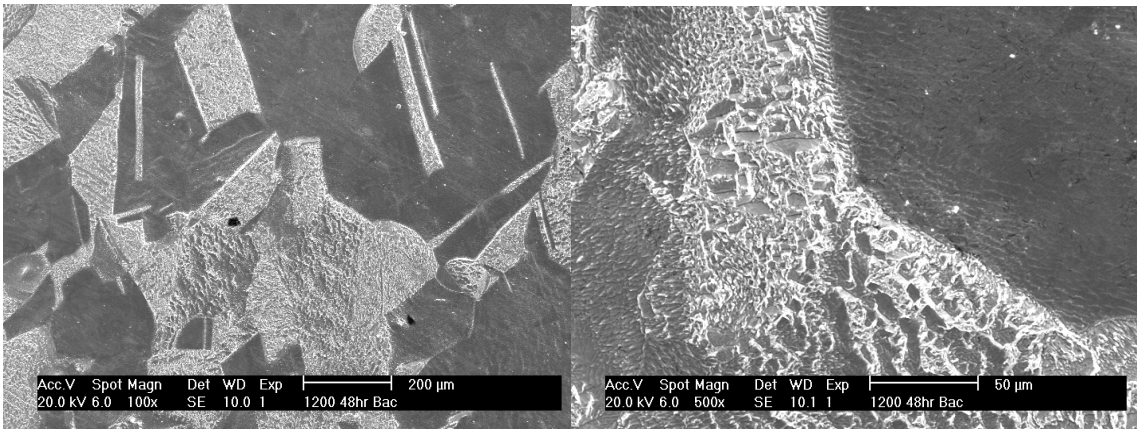

1200 Finish, 48 Hour, With Bacteria

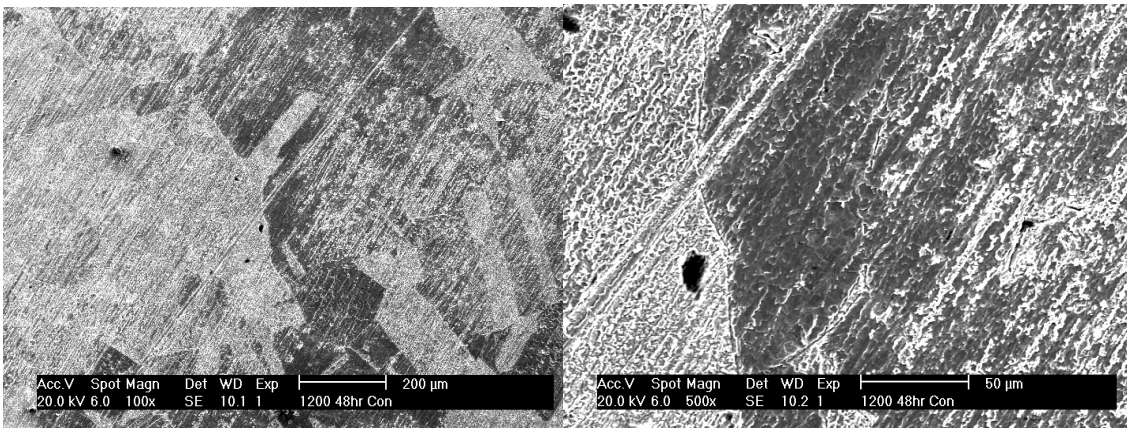

1200, 48 Hour, Control

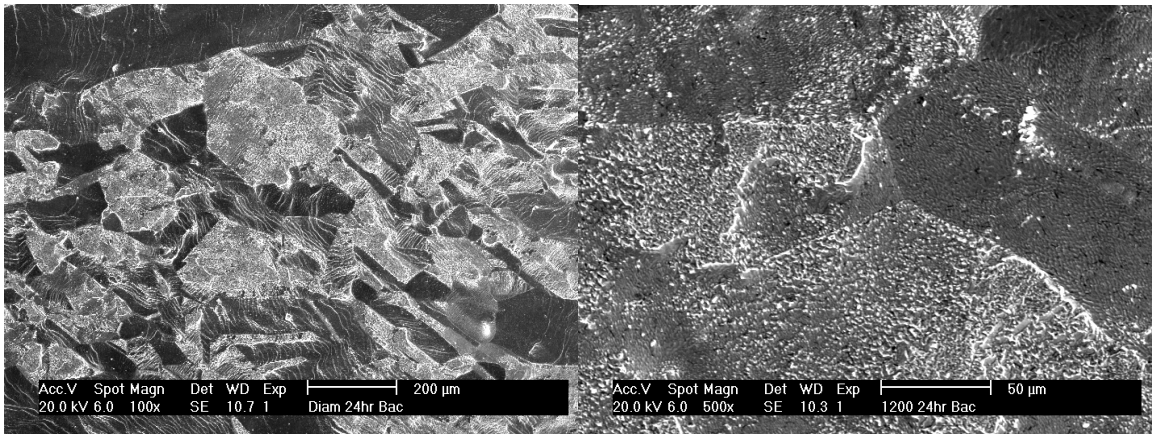

.6µm Diamond Finish, 24 Hour, With Bacteria

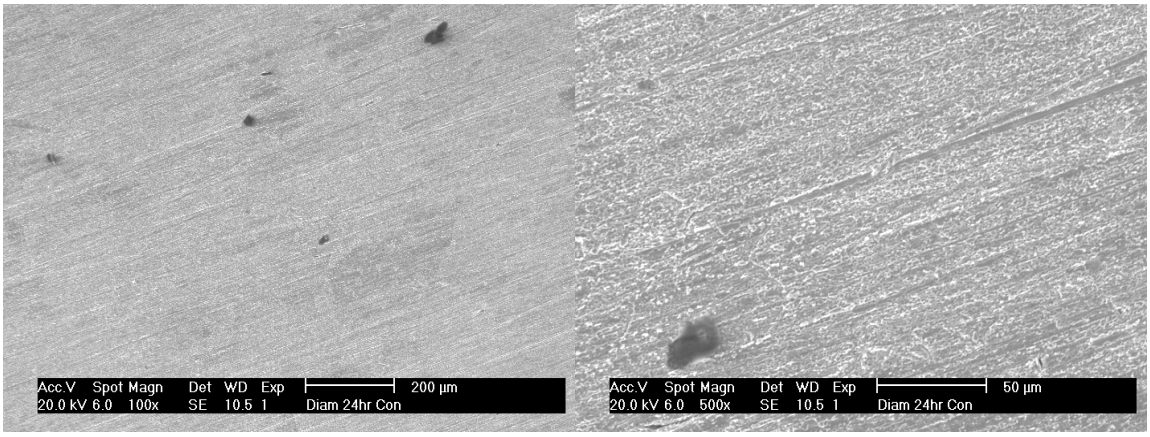

.6µm Diamond Finish, 24 Hour, Control

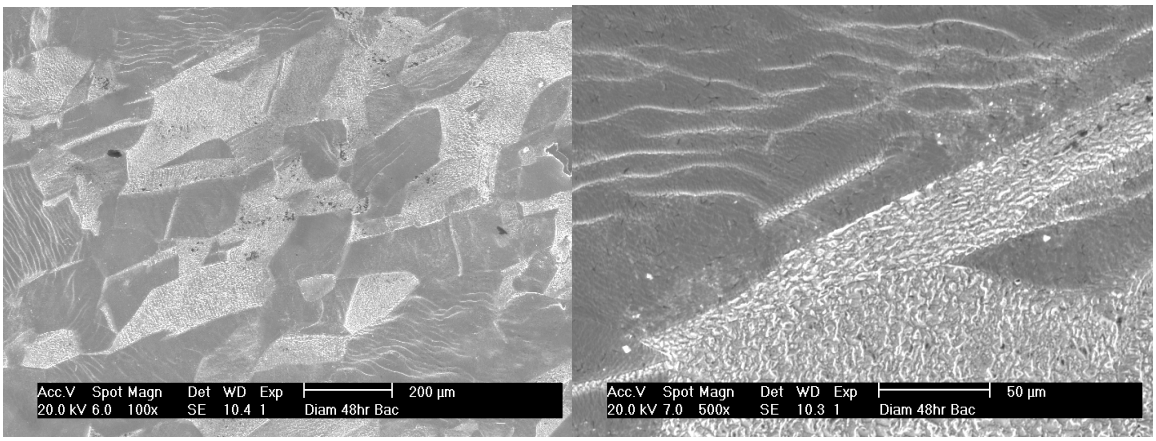

.6µm Diamond Finish, 48 Hour, With Bacteria

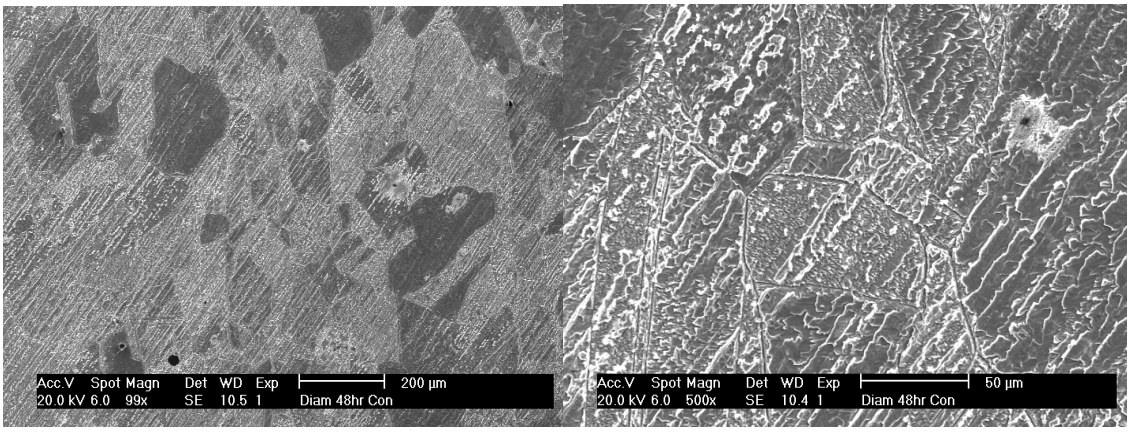

.6µm Diamond Finish, 48 Hour, Control